Journal of Chemical&Engineering Data

pubs.acs.org/jced Article

Densities, Viscosities, and Self-Diffusion Coefficients of Ethylene Glycol Oligomers

Markus M. Hoffmann,* Rachel H. Horowitz, Torsten Gutmann, and Gerd Buntkowsky*

Cite This: J. Chem. Eng. Data 2021, 66, 2480−2500 Read Online

ACCESS | Metrics & More | Article Recommendations | Supporting Information

ABSTRACT: Polyethylene glycol (PEG) is gaining interest as an alternative green solvent in chemical synthesis and processing. This report presents density and viscosity data from 293.15 K to 358.15 K as well as self-diffusion coefficient data from 298.15 K to 358.15 K for oligomers of PEG from di- to nonaethylene glycol. The results were obtained by extrapolation from measurement series where water, the most common impurity in PEGs, was intentionally added in several increments. The obtained results are carefully compared to literature data, which are widely available only for density and viscosity, and only for the lower oligomers. Densities are found to be linearly dependent on temperatures for all studied oligomers. The temperature dependence of viscosity and self-diffusion coefficients show only slight deviations from the Arrhenius equation over the investigated temperature range. The activation energies obtained from the viscosity data agree well with the activation energies from the self-diffusion coefficient data and appear to be linearly dependent with respect to the number of ethylene oxide repeat units in the PEG oligomer. This linearity combined with the observation that the pre-exponential factor appears to be the same for all studied oligomers may serve as a tool to estimate viscosities and self-diffusion coefficients for higher oligomers within the investigated temperature range. The densities of the oligomers all fall within a rather narrow range without a clear trend in homologous series.

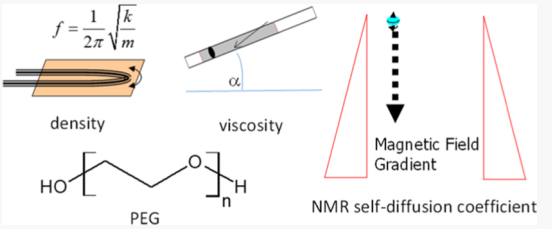

1. INTRODUCTION

Polyethylene glycol (PEG, $H-[O-CH_2-CH_2]_n-OH$) is industrially produced for a variety of applications, mostly in the personal and health care industries.[1−3] Industrially produced PEG is polydisperse with the average molar mass indicated as part of the product name such as PEG 400, where 400 g/mol is the average molar mass. Given that low molar mass PEGs (<1000 $g \cdot mol^{-1}$) are liquid at room temperature and that PEG is nontoxic, harmless to the environment and biodegradable,[4] PEG has been recognized as a promising solvent for chemical synthesis for quite some time. Early works have been reviewed in 2005.[5,6] Since then, much progress has been made. Especially, one-pot synthesis type reactions, where many different components react in one step, have been successfully carried out in PEG due to its ability to dissolve a wide range of compounds.[7−11] In fact, PEG can also dissolve mineral salts,[5,12] a contributing factor for its successful use as the reaction medium for the synthesis of metal−organic frameworks.[13] Pd-catalyzed reactions (the importance of these can be seen in the 2010 Nobel prize award for their discovery[14]) have also been carried out in PEG under both homocatalytic and heterocatalytic conditions where Pd is immobilized onto a porous silica material.[15−19] PEGs have also been successfully used as components in deep eutectic solvents.[20−27] Despite all of these successes, there are only limited experimental and theoretical studies on the dynamics of neat PEG.[28−30] Experimental physicochemical properties of PEGs are needed to further this effort. In this respect, densities and viscosities have been repeatedly reported for several polydisperse PEGs usually as part of studies on binary mixtures involving polydisperse PEGs.[31−83] The polydisperse PEGs are composed of mixtures of PEG oligomers with approximately a Gaussian mole fraction distribution around the mean chain length.[60,84,85] It is likely that the exact mole fraction distribution may vary from vendor to vendor and possibly even from batch to batch. Unfortunately, a composition analysis of polydisperse PEGs is typically not included in the above cited studies. In this regard, it would be helpful if one could predict the physicochemical properties of polydisperse PEGs based on the analysis of their exact composition. It should be noted that even the low average molar mass PEG 200 covers oligomers from mono- to nonaethylene glycol with tetra- and pentaethylene glycol being the most prominent components.[84,85] A perusal of the literature reveals that there are numerous reports on density and viscosity for the neat lowest oligomers diethylene glycol,[23,25,58−62,86−126] triethylene glycol,[23,58−60,62,95,96,100−102,104−110,112−118,121−140] and tetraethylene glycol,[62,95,100,101,104−107,110,112,116−118,120−126,129−131,140] but re-

Received: February 8, 2021
Accepted: April 22, 2021
Published: May 5, 2021

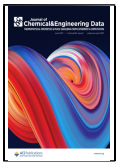

https://doi.org/10.1021/acs.jced.1c00101
J. Chem. Eng. Data 2021, 66, 2480−2500

ports are scarce or absent for pentaethyelene glycol[101,126] and higher oligomers.[101,126,141] As for self-diffusion coefficients, we are not aware of any reports on neat oligomers nor on polydisperse PEG. We are only aware of self-diffusion measurements of PEGs as part of bi- or multi-component systems.[142−144] Thus, the motivation of this study is to address this lack of data by measuring density, viscosity, and self-diffusion coefficient of the PEG oligomers from di- to nonaethylene glycol over a wide range of temperatures. To this effect, it is important to recognize that PEGs readily absorb water from the atmosphere. Rather than drying PEGs to remove as much as possible any water contamination, we took the approach of purposely adding incrementally water. Back extrapolating to zero water content then establishes the physicochemical property values of the neat PEGs. Hence, this study includes inspection of the effect of present water impurity on the physicochemical properties, which, to the best of our knowledge, has not been done before.

2. EXPERIMENTAL SECTION

2.1. Preparation of Samples. Samples of polyethylene glycol components were prepared in order to test the effect of water content on the physicochemical properties of density, viscosity, and self-diffusion coefficient. For each sample, the density, viscosity, and self-diffusion coefficient were measured. The vendors and purities of the polyethylene glycol components and other chemicals used are shown in Table 1. The chemicals were used as received without further purification, although a light brown tint was observed for triethylene and pentaethylene glycol. The glycols were generally handled and stored under dry nitrogen in a glovebox to ensure that no additional water would be absorbed from the outside air. The water content of the neat samples was tested in triplicate using a fritless C20 Mettler Toledo Karl Fischer (KF) titrator.

Table 1. Information on Chemicals Used

chemical name	CAS	source	mass fraction purity[a]
diethylene glycol	111-46-6	Alfa Aesar	0.99
triethylene glycol	112-27-6	Alfa Aesar	0.99
tetraethylene glycol	112-60-7	Acros Organics	0.995
pentaethylene glycol	4792-15-8	Alfa Aesar	0.98+
hexaethylene glycol	2615-15-8	TCI	>0.98
heptaethylene glycol	5617-32-3	Broadpharm	0.993
octanethyl glycol	5117-19-1	Broadpharm	0.991
nonaethylene glycol	3386-18-3	Broadpharm	0.996
water	7732-18-5	Anton Paar	"ultra-pure"
S60 viscosity/density standard	8042-47-3	Koehler	not applicable[b]
S60 viscosity/density standard	64742-54-7	Cannon Instrument Company	not applicable[b]
APN 26 viscosity/density standard		Anton Paar	not applicable[b]

[a]As stated by the vendor, no further mass fraction purity determination was done other than KF water content analysis as reported in Section 3. [b]Standards only come with provided certified density and viscosity measurements.

An analytical balance (±0.0001 g) was used for all mass measurements for both KF titrations and sample preparation. The standard deviations of the KF measurements were within 10% relative standard deviation (RSD). Samples where no additional water was added were handled entirely in the glovebox. Addition of water was done outside of the glovebox where exposure to an open atmosphere was less than 2 min before the sample received the added water. The approach to adding water was different for the more expensive pentaethylene to nonaethylene glycol compared to diethylene to tetraethylene glycol. Diethylene to tetraethylene glycol samples were discarded after each set of measurement, and sample preparation was conducted anew where, in a 20 mL vial, the amount of needed water was added to about 5 mL of the neat glycol. The vial was then vigorously shaken for approximately 1 min to ensure homogeneity. Pentaethylene to nonaethylene glycol samples were recovered after each set of measurement, and water was added to the recovered sample. The water content of each sample was calculated based on the mass of the recovered sample, its water content before adding additional water, and the mass of added water. The water content was spot checked by KF titrations for some samples, and agreement was within the above stated 10% RSD.

2.2. Density and Viscosity Measurements. Densities and viscosities were measured the same day samples were prepared. Densities and viscosities were measured in parallel using two different vibrating tube density meters and rolling ball viscometers all manufactured by Anton Paar and all with Peltier temperature controls stated to have an accuracy of 0.02 K. The densities and viscosities of samples with diethylene to hexaethylene glycol were measured with the models DMA 4100 and AMVn automated micro viscometer. For samples with heptaethylene to nonaethylene glycol, the models DMA 4100 M and Lovis 2000 M/ME were used for density and viscosity measurements, respectively. Both density meters apply internal corrections for viscosity effects during measurements. The samples are enclosed in either a measuring cell or capped capillaries for density and viscosity measurements, respectively. The capillary diameter was 1.8 mm for both viscometer models. Measurements were repeated at least six times for each temperature setting. Each temperature cycle started at 20 °C, increased to 85 °C in 5 °C increments, and cooled back to 20 °C. Measurements from initial and final 20 °C settings agreed within measurement uncertainty. The density and viscosity instruments were calibrated and accuracy checked with standard oils listed in Table 1. Agreement between the two sets of Anton Paar instruments was ascertained with several tetraethylene glycol samples. The standard deviations for the viscosities measured with the AMVn viscometer are reported in Table S1. The Lovis 2000 M/ME viscometer does not report the results from each individual measurement repetition but only the average values. However, the instrument reports the variation coefficients, which were always less than 1%, typically less than 0.1%. The standard deviations for the density measurements with the DMV 4100 instrument were within 0.0002 $g \cdot cm^{-3}$, and similar precision is assumed to apply also for the DMV 4100 M instrument. However, the standard uncertainty of the density measurement is actually limited by the sample mass fraction purities listed in Table 1, for which a relative uncertainty of 0.1% is appropriate. This sets the standard uncertainty for density measurements to 0.001 $g \cdot cm^{-3}$.

2.3. Self-Diffusion Coefficient Measurements. The instrument used for all NMR measurements was a Bruker Avance 300 NMR spectrometer. The temperature of the variable temperature broadband probe was calibrated against known chemical shifts of ethylene glycol,[145] where standard uncertainty is estimated to be 0.3 K. Each sample was transferred into a

https://doi.org/10.1021/acs.jced.1c00101
J. Chem. Eng. Data 2021, 66, 2480−2500

Table 2. Density, Viscosity, and Self-Diffusion Coefficient of Diethylene Glycol with Small Amounts of Water in 10^{-6} Mass Fraction, w, as well as Mole Fraction, x_w, Present at Ambient Pressure (0.10 ± 0.01 MPa)[a]

	$w/10^{-6}$							
	2192	6469	6521	6733	13,594	15,023		
	x_w							
T/K	0.013	0.037	0.037	0.038	0.075	0.082	slope	intercept
	Density/10^{-3} kg·m^{-3}						10^{-3} kg·m^{-3}	10^{-3} kg·m^{-3}
293.15	1.1166	1.1166	1.1165	1.1165	1.1163	1.1152	−0.09 ± 0.03	1.1170 ± 0.0003
298.15	1.1132	1.1133	1.1132	1.1132	1.1130	1.1115	−0.10 ± 0.05	1.1138 ± 0.0005
303.15	1.1096	1.1097	1.1096	1.1096	1.1094	1.1080	−0.10 ± 0.04	1.1101 ± 0.0004
308.15	1.1060	1.1061	1.1060	1.1060	1.1057	1.1046	−0.09 ± 0.04	1.1065 ± 0.0003
313.15	1.1023	1.1025	1.1023	1.1023	1.1021	1.1011	−0.08 ± 0.03	1.1028 ± 0.0003
318.15	1.0987	1.0988	1.0987	1.0987	1.0985	1.0977	−0.07 ± 0.03	1.0991 ± 0.0003
323.15	1.0950	1.0952	1.0950	1.0950	1.0948	1.0942	−0.06 ± 0.02	1.0953 ± 0.0002
328.15	1.0914	1.0915	1.0914	1.0914	1.0911	1.0907	−0.05 ± 0.02	1.0917 ± 0.0001
333.15	1.0877	1.0878	1.0877	1.0877	1.0874	1.0871	−0.05 ± 0.01	1.0880 ± 0.0001
338.15	1.0840	1.0841	1.0840	1.0840	1.0837	1.0835	−0.04 ± 0.01	1.0842 ± 0.0001
343.15	1.0803	1.0804	1.0803	1.0802	1.0800	1.0798	−0.04 ± 0.01	1.0805 ± 0.0001
348.15	1.0765	1.0766	1.0765	1.0765	1.0762	1.0761	−0.04 ± 0.01	1.0767 ± 0.0001
353.15	1.0727	1.0728	1.0727	1.0727	1.0724	1.0723	−0.04 ± 0.01	1.0729 ± 0.0001
358.15	1.0689	1.0690	1.0689	1.0689	1.0686	1.0684	−0.04 ± 0.01	1.0691 ± 0.0001
	Viscosity/mPa·s						10^2 mPa·s	mPa·s
293.15	37.311	35.381	33.153	34.695	34.974	34.545	−1.2 ± 1.3	36.0 ± 1.2
298.15	29.024	27.760	25.762	27.253	27.472	27.116	−0.8 ± 1.0	28.0 ± 1.0
303.15	23.059	22.206	20.642	21.920	21.954	21.704	−0.5 ± 0.8	22.4 ± 0.7
308.15	18.686	18.114	16.841	17.884	17.921	17.699	−0.4 ± 0.6	18.2 ± 0.6
313.15	15.385	14.964	13.922	15.254	14.798	14.608	−0.4 ± 0.5	15.1 ± 0.5
318.15	12.838	12.509	11.669	12.405	12.367	12.237	−0.2 ± 0.4	12.5 ± 0.4
323.15	10.846	10.576	9.873	10.495	10.435	10.346	−0.2 ± 0.3	10.6 ± 0.3
328.15	9.254	9.035	8.426	8.953	8.892	8.833	−0.2 ± 0.3	9.0 ± 0.3
333.15	7.939	7.708	7.345	7.635	7.582	7.544	−0.2 ± 0.2	7.8 ± 0.2
338.15	6.866	6.697	6.263	6.632	6.586	6.551	−0.1 ± 0.2	6.7 ± 0.2
343.15	6.054	5.936	5.553	5.884	5.824	5.814	−0.1 ± 0.2	5.9 ± 0.2
348.15	5.235	5.262	4.922	5.217	5.169	5.153	0.0 ± 0.1	5.2 ± 0.1
353.15	4.522	4.530	4.245	4.506	4.447	4.439	0.0 ± 0.1	4.5 ± 0.1
358.15	3.944	4.046	3.800	4.026	3.974	3.966	0.02 ± 0.09	3.9 ± 0.1
	Self-diffusion coefficient/10^{-10} m^2·s^{-1}						10^{-10} m^2·s^{-1}	10^{-10} m^2·s^{-1}
298.15	0.595		0.536	0.530	0.536	0.530	−0.4 ± 0.2	0.58 ± 0.02
303.15	0.687	0.680	0.660	0.661	0.677	0.666	−0.1 ± 0.1	0.68 ± 0.01
308.15	0.795	0.843	0.830	0.827	0.856	0.836	0.3 ± 0.1	0.80 ± 0.01
313.15	1.012	1.076	1.027	1.027	1.022	1.037	0.0 ± 0.2	1.03 ± 0.02
318.15	1.243	1.297	1.227	1.230	1.241	1.245	0.0 ± 0.3	1.25 ± 0.02
323.15	1.465	1.549	1.472	1.487	1.512	1.500	0.2 ± 0.3	1.48 ± 0.03
328.15	1.684	1.866	1.789	1.761	1.776	1.796	0.4 ± 0.6	1.74 ± 0.05
333.15	2.007	2.147	2.029	2.040	2.083	2.114	0.6 ± 0.5	2.02 ± 0.04
338.15	2.293	2.458	2.366	2.335	2.434	2.405	0.8 ± 0.5	2.32 ± 0.05
343.15	2.619	2.837	2.697	2.706	2.823	2.770	1.1 ± 0.6	2.65 ± 0.06
348.15	2.995	3.418	3.102	3.059	3.178	3.146	0.7 ± 1.5	3.09 ± 0.14
353.15	3.484	3.771	3.602	3.587	3.668	3.560	0.4 ± 1.0	3.58 ± 0.09
358.15	4.032	4.184	4.013	4.052	4.090	4.081	0.3 ± 0.6	4.05 ± 0.06

[a]Relative standard uncertainty of w and x_w is 0.05. Temperature standard uncertainty is estimated to be 0.02 K for the density and viscosity measurements and 0.3 K for the self-diffusion coefficient measurements. The shown standard deviations of the intercepts provide an estimate for the standard uncertainty of viscosity and self-diffusion coefficient, whereas for density, the relative standard uncertainty is limited by sample impurity to 0.001.

melting tube capillary using a syringe with a blunt gauge-20 stainless steel needle and then immediately flame sealed. The flame sealed capillary was inserted into a standard 5 mm NMR tube to which a deuterated solvent was added (typically DMSO-d_6 and for some samples D_2O). During a measurement series, the NMR tube was not spun and the temperature was equilibrated for at least 20 min. As pulse program for the self-diffusion measurements, a double stimulated echo with bipolar gradients and 3 spoiler gradients was used[146,147] with the following settings: 5 s relaxation delay, 5 ms eddy current recovery, and 0.2 ms gradient recovery. The obtained stimulated spin-echo intensity, $I(g)$, for each of the two CH_2 signals was found by integrating the respective spectral peak and then fitted

https://doi.org/10.1021/acs.jced.1c00101
J. Chem. Eng. Data 2021, 66, 2480−2500

Table 3. Density, Viscosity, and Self-Diffusion Coefficient of Triethylene Glycol with Small Amounts of Water in 10^{-6} Mass Fraction, w, as well as Mole Fraction, x_w, Present at Ambient Pressure (0.10 ± 0.01 MPa)[a]

	$w/10^{-6}$					
	1655	6269	12,340	14,947		
	x_w					
T/K	0.014	0.050	0.094	0.112	slope	intercept
	Density/10^{-3} kg·m^{-3}				10^{-5} kg·m^{-3}	10^{-3} kg·m^{-3}
293.15	1.1242	1.1242	1.1239	1.1238	−3.3 ± 0.8	1.1243 ± 0.0001
298.15	1.1206	1.1205	1.1202	1.1202	−3.4 ± 0.5	1.1207 ± 0.0001
303.15	1.1166	1.1166	1.1163	1.1162	−3.3 ± 0.8	1.1167 ± 0.0001
308.15	1.1127	1.1127	1.1124	1.1123	−3.3 ± 0.8	1.1128 ± 0.0001
313.15	1.1088	1.1087	1.1084	1.1084	−3.3 ± 0.4	1.10887 ± 0.00004
318.15	1.1049	1.1048	1.1045	1.1045	−3.4 ± 0.5	1.1050 ± 0.0001
323.15	1.1009	1.1009	1.1006	1.1005	−3.3 ± 0.8	1.1010 ± 0.0001
328.15	1.0970	1.0969	1.0967	1.0966	−3.0 ± 0.2	1.09707 ± 0.00002
333.15	1.0930	1.0930	1.0927	1.0926	−3.3 ± 0.8	1.0931 ± 0.0001
338.15	1.0891	1.0890	1.0887	1.0887	−3.3 ± 0.5	1.08917 ± 0.00005
343.15	1.0851	1.0850	1.0848	1.0847	−3.1 ± 0.4	1.08519 ± 0.00005
348.15	1.0811	1.0811	1.0808	1.0807	−3.3 ± 0.8	1.0812 ± 0.0001
353.15	1.0771	1.0771	1.0768	1.0767	−3.3 ± 0.8	1.0772 ± 0.0001
358.15	1.0731	1.0730	1.0727	1.0727	−3.3 ± 0.4	1.07318 ± 0.00004
	Viscosity/mPa·s				10^2 mPa·s	mPa·s
293.15	47.578	46.031	44.796	45.719	−1.6 ± 0.8	47.4 ± 0.8
298.15	37.144	35.944	34.657	35.507	−1.5 ± 0.6	37.1 ± 0.7
303.15	29.253	28.191	27.247	27.951	−1.2 ± 0.5	29.2 ± 0.6
308.15	23.516	22.552	21.884	22.444	−0.9 ± 0.5	23.4 ± 0.5
313.15	19.226	18.393	17.834	18.290	−0.8 ± 0.4	19.1 ± 0.4
318.15	15.908	15.201	14.729	15.129	−0.7 ± 0.3	15.8 ± 0.3
323.15	13.327	12.703	12.324	12.644	−0.6 ± 0.3	13.3 ± 0.3
328.15	11.280	10.771	10.426	10.700	−0.5 ± 0.2	11.2 ± 0.2
333.15	9.590	9.130	8.849	9.067	−0.4 ± 0.2	9.5 ± 0.2
338.15	8.274	7.875	7.637	7.820	−0.4 ± 0.2	8.2 ± 0.2
343.15	7.269	6.950	6.731	6.894	−0.3 ± 0.1	7.2 ± 0.1
348.15	6.411	6.128	5.932	6.075	−0.3 ± 0.1	6.4 ± 0.1
353.15	5.527	5.235	5.101	5.205	−0.3 ± 0.1	5.5 ± 0.1
358.15	4.916	4.648	4.540	4.626	−0.2 ± 0.1	4.9 ± 0.1
	Self-diffusion coefficient/10^{-10} m^2·s^{-1}				10^{-10} m^2·s^{-1}	10^{-10} m^2·s^{-1}
298.15	0.368	0.376	0.385	0.382	1.1 ± 0.3	0.368 ± 0.003
303.15	0.472	0.474	0.491	0.479	1.0 ± 0.7	0.470 ± 0.007
308.15	0.592	0.597	0.611	0.609	1.4 ± 0.3	0.590 ± 0.003
313.15	0.720	0.751	0.747	0.751	2 ± 1	0.73 ± 0.01
318.15	0.883	0.916	0.919	0.913	2 ± 1	0.89 ± 0.01
323.15	1.056	1.103	1.111	1.116	4 ± 1	1.06 ± 0.01
328.15	1.268	1.280	1.327	1.363	7 ± 1	1.25 ± 0.01
333.15	1.499	1.549	1.563	1.613	7 ± 2	1.49 ± 0.02
338.15	1.810	1.844	1.814	1.837	1 ± 2	1.82 ± 0.02
343.15	2.015	2.174	2.097	2.105	4 ± 7	2.06 ± 0.07
348.15	2.287	2.405	2.422	2.447	11 ± 3	2.29 ± 0.04
353.15	2.633	2.648	2.763	2.676	6 ± 5	2.62 ± 0.05
358.15	3.135	3.129	3.156	3.244	7 ± 4	3.10 ± 0.04

[a]Relative standard uncertainty of w and x_w is 0.05. Temperature standard uncertainty is estimated to be 0.02 K for the density and viscosity measurements and 0.3 K for the self-diffusion coefficient measurements. The shown standard deviations of the intercepts provide an estimate for the standard uncertainty of viscosity and self-diffusion coefficient, whereas for density, the relative standard uncertainty is limited by sample impurity to 0.001.

as a function of magnetic field gradient strength, g, according to the equation[148]

$$I(g) = I_0 e^{-D\gamma^2 g^2 \delta^2 ((4\Delta - \delta)/\pi^2)} \quad (1)$$

where I_0 is the reference spin-echo intensity in the absence of a gradient, γ is the ^{1}H gyromagnetic ratio, and Δ is the diffusion time of 0.1 s. The length of the sine-shaped gradient pulse, δ, was optimized for each sample and temperature condition. In each self-diffusion measurement, the field gradient strength was varied by a total of 16 different linearly incremented values ranging from 0.48 to 4.8 G·mm^{-1}. Four dummy scans were used prior to the 16 scans to acquire steady-state conditions. The

https://doi.org/10.1021/acs.jced.1c00101
J. Chem. Eng. Data 2021, 66, 2480−2500

Table 4. Density, Viscosity, and Self-Diffusion Coefficient of Tetraethylene Glycol with Small Amounts of Water in 10^{-6} Mass Fraction, w, as well as Mole Fraction, x_w, Present at Ambient Pressure (0.10 ± 0.01 MPa)[a]

	$w/10^{-6}$									
	1308	5463	5776	6438	9687	10,249	13,340	14,978		
	x_w									
T/K	0.014	0.056	0.059	0.065	0.095	0.100	0.127	0.141	slope	intercept
	Density/10^{-3} kg·m^{-3}								10^{-5} kg·m^{-3}	10^{-3} kg·m^{-3}
293.15	1.1237	1.1237	1.1238	1.1238	1.1236	1.1226	1.1235	1.1235	−3 ± 3	1.1238 ± 0.0003
298.15	1.1199	1.1200	1.1200	1.1200	1.1199	1.1186	1.1197	1.1198	−3 ± 4	1.1200 ± 0.0004
303.15	1.1159	1.1160	1.1160	1.1160	1.1159	1.1150	1.1157	1.1158	−3 ± 3	1.1160 ± 0.0003
308.15	1.1119	1.1120	1.1120	1.1120	1.1119	1.1113	1.1118	1.1118	−2 ± 2	1.1120 ± 0.0002
313.15	1.1078	1.1080	1.1080	1.1080	1.1079	1.1076	1.1078	1.1078	−1 ± 1	1.1080 ± 0.0001
318.15	1.1038	1.1040	1.1040	1.1040	1.1039	1.1037	1.1038	1.1038	−1 ± 1	1.1040 ± 0.0001
323.15	1.0998	1.1000	1.1000	1.1000	1.0999	1.0998	1.0998	1.0998	−1.0 ± 0.8	1.0010 ± 0.0001
328.15	1.0958	1.0960	1.0960	1.0960	1.0959	1.0958	1.0958	1.0958	−1.0 ± 0.8	1.0960 ± 0.0001
333.15	1.0918	1.0920	1.0920	1.0920	1.0919	1.0919	1.0918	1.0918	−0.8 ± 0.8	1.0920 ± 0.0001
338.15	1.0878	1.0880	1.0880	1.0879	1.0879	1.0879	1.0878	1.0878	−0.7 ± 0.7	1.0880 ± 0.0001
343.15	1.0838	1.0839	1.0840	1.0839	1.0839	1.0838	1.0838	1.0838	−0.6 ± 0.6	1.0839 ± 0.0001
348.15	1.0798	1.0799	1.0799	1.0799	1.0798	1.0798	1.0798	1.0797	−0.9 ± 0.5	1.0799 ± 0.0001
353.15	1.0758	1.0759	1.0759	1.0759	1.0758	1.0758	1.0758	1.0757	−1.2 ± 0.5	1.0759 ± 0.0001
358.15	1.0718	1.0719	1.0719	1.0719	1.0718	1.0718	1.0717	1.0717	−1.3 ± 0.5	1.0719 ± 0.0001
	Viscosity/mPa·s								10^2 mPa·s	mPa·s
293.15	57.681	57.005	59.985	56.558	58.762	58.333	58.171	52.996	−1.9 ± 1.7	59.1 ± 1.6
298.15	43.779	45.217	46.118	43.890	45.023	44.784	44.431	41.148	−1.5 ± 1.2	45.6 ± 1.1
303.15	34.056	35.364	35.964	34.348	35.259	35.037	34.740	32.095	−1.1 ± 1.0	35.5 ± 0.9
308.15	27.108	28.199	28.593	27.455	28.079	27.949	27.735	25.578	−0.8 ± 0.8	28.3 ± 0.7
313.15	21.929	22.874	23.133	22.315	22.770	22.700	22.516	20.756	−0.6 ± 0.6	22.9 ± 0.6
318.15	18.015	18.846	19.025	18.378	18.733	18.684	18.534	17.092	−0.5 ± 0.5	18.8 ± 0.5
323.15	14.993	15.740	15.849	15.336	15.622	15.594	15.474	14.274	−0.4 ± 0.4	15.7 ± 0.4
328.15	12.645	13.284	13.378	12.955	13.196	13.167	13.067	12.046	−0.3 ± 0.4	13.2 ± 0.3
333.15	10.755	11.277	11.348	11.000	11.212	11.186	11.092	10.204	−0.3 ± 0.3	11.3 ± 0.3
338.15	9.266	9.725	9.786	9.487	9.668	9.647	9.571	8.787	−0.3 ± 0.3	9.7 ± 0.3
343.15	8.115	8.559	8.605	8.352	8.500	8.478	8.413	7.727	−0.2 ± 0.2	8.5 ± 0.2
348.15	7.123	7.537	7.587	7.359	7.484	7.474	7.413	6.806	−0.2 ± 0.2	7.5 ± 0.2
353.15	6.156	6.492	6.533	6.341	6.450	6.445	6.389	5.852	−0.2 ± 0.2	6.5 ± 0.2
358.15	5.461	5.769	5.803	5.637	5.735	5.726		5.201	−0.2 ± 0.2	5.8 ± 0.2
	Self-diffusion coefficient/10^{-10} m^2·s^{-1}								10^{-10} m^2·s^{-1}	10^{-10} m^2·s^{-1}
298.15	0.297	0.299		0.305	0.295	0.453	0.288	0.305	0.2 ± 0.6	0.31 ± 0.05
303.15	0.377	0.381	0.347	0.385	0.380	0.472	0.356	0.362	0.0 ± 0.3	0.38 ± 0.03
308.15	0.470	0.435	0.435	0.476	0.521	0.602	0.449	0.449	0.2 ± 0.5	0.46 ± 0.05
313.15	0.585	0.555	0.559	0.598	0.559	0.767	0.576	0.578	0.2 ± 0.6	0.58 ± 0.06
318.15	0.719	0.677	0.690	0.735	0.705	0.949	0.710	0.705	0.3 ± 0.8	0.71 ± 0.07
323.15	0.872	0.816	0.829	0.875	0.844	1.131	0.853	0.882	0.5 ± 0.9	0.85 ± 0.08
328.15	1.034	0.989	1.010	1.047	1.042	1.374	1.038	1.050	0.7 ± 1.1	1.0 ± 0.1
333.15	1.220	1.177	1.195	1.239	1.243	1.662	1.233	1.260	0.9 ± 1.4	1.2 ± 0.1
338.15	1.449	1.377	1.410	1.449	1.418	1.890	1.401	1.462	0.7 ± 1.5	1.4 ± 0.1
343.15	1.652	1.663	1.683	1.693	1.611	2.146	1.615	1.668	0.4 ± 1.6	1.7 ± 0.1
348.15	1.858	1.835	1.861	1.879	1.931	2.603	1.937	2.011	2.0 ± 2.1	1.8 ± 0.2
353.15	2.128	2.199	2.272	2.165	2.217	2.980	2.234	2.278	1.8 ± 2.4	2.2 ± 0.2
358.15	2.401	2.424	2.374	2.451	2.385	3.171	2.462	2.591	2.0 ± 2.3	2.4 ± 0.2

[a]Relative standard uncertainty of w and x_w is 0.05. Temperature standard uncertainty is estimated to be 0.02 K for the density and viscosity measurements and 0.3 K for the self-diffusion coefficient measurements. The shown standard deviations of the intercepts provide an estimate for the standard uncertainty of viscosity and self-diffusion coefficient, whereas for density, the relative standard uncertainty is limited by sample impurity to 0.001.

reported PEG self-diffusion coefficients were determined as the average from the two PEG CH_2 signals. Tables S2.

3. RESULTS AND DISCUSSION

3.1. Water Content Dependence. Tables 2−9 summarize all measurement results for density, viscosity, and self-diffusion coefficient for di- to nonaethylene glycol at ambient pressure (~0.1 MPa) with varying water contents (columns) and temperatures (rows). A few self-diffusion coefficient entries at 298.15 K are missing because of inadvertent loss of the sample capillary. The water content in Tables 2−9 is expressed as reported by the KF titrator instrument, i.e., as mass fraction, w (the instrument reports in parts per million, ppm = 10^{-6}). Water

https://doi.org/10.1021/acs.jced.1c00101
J. Chem. Eng. Data 2021, 66, 2480−2500

Table 5. Density, Viscosity, and Self-Diffusion Coefficient of Pentaethylene Glycol with Small Amounts of Water in 10^{-6} Mass Fraction, w, as well as Mole Fraction, x_w, Present at Ambient Pressure (0.10 ± 0.01 MPa)[a]

	$w/10^{-6}$					
	1798	6592	12,532	14,816		
	x_w					
T/K	0.023	0.081	0.144	0.166	slope	intercept
	Density/10^{-3} kg·m^{-3}				10^{-4} kg·m^{-3}	10^{-3} kg·m^{-3}
293.15	1.1253	1.1249	1.1245	1.1240	−0.9 ± 0.2	1.1255 ± 0.0002
298.15	1.1214	1.1211	1.1207	1.1201	−0.9 ± 0.2	1.1216 ± 0.0002
303.15	1.1174	1.1171	1.1166	1.1161	−0.9 ± 0.2	1.1176 ± 0.0002
308.15	1.1133	1.1130	1.1126	1.1120	−0.9 ± 0.2	1.1135 ± 0.0002
313.15	1.1093	1.1090	1.1085	1.1080	−0.9 ± 0.2	1.1095 ± 0.0002
318.15	1.1052	1.1049	1.1045	1.1039	−0.9 ± 0.2	1.1055 ± 0.0002
323.15	1.1012	1.1009	1.1004	1.0999	−0.9 ± 0.2	1.1014 ± 0.0002
328.15	1.0971	1.0968	1.0964	1.0958	−0.9 ± 0.2	1.0974 ± 0.0002
333.15	1.0931	1.0927	1.0923	1.0917	−1 ± 0.2	1.0933 ± 0.0002
338.15	1.0891	1.0887	1.0882	1.0877	−1 ± 0.1	1.0893 ± 0.0001
343.15	1.0850	1.0846	1.0841	1.0836	−1 ± 0.1	1.0852 ± 0.0002
348.15	1.0810	1.0805	1.0801	1.0796	−1 ± 0.2	1.0812 ± 0.0002
353.15	1.0769	1.0765	1.0760	1.0755	−1 ± 0.1	1.0771 ± 0.0001
358.15	1.0728	1.0724	1.0719	1.0714	−1 ± 0.1	1.0730 ± 0.0001
	Viscosity/mPa·s				10^2 mPa·s	mPa·s
293.15	70.879	72.825	71.378	70.737	−0.3 ± 1.1	71.8 ± 1.2
298.15	54.118	55.716	54.328	53.661	−0.5 ± 1.0	54.9 ± 1.0
303.15	42.277	43.212	42.276	41.757	−0.5 ± 0.6	42.8 ± 0.7
308.15	33.634	34.210	33.532	33.102	−0.5 ± 0.4	34.0 ± 0.5
313.15	27.216	27.554	27.007	26.669	−0.5 ± 0.3	27.5 ± 0.3
318.15	22.338	22.558	22.113	21.833	−0.4 ± 0.2	22.6 ± 0.2
323.15	18.573	18.680	18.336	18.076	−0.4 ± 0.2	18.8 ± 0.2
328.15	15.644	15.682	15.386	15.149	−0.4 ± 0.1	15.8 ± 0.1
333.15	13.276	13.268	13.030	12.822	−0.3 ± 0.1	13.4 ± 0.1
338.15	11.431	11.393	11.182	10.993	−0.3 ± 0.1	11.5 ± 0.1
343.15	10.029	9.946	9.765	9.583	−0.3 ± 0.1	10.1 ± 0.1
348.15	8.827	8.734	8.593	8.417	−0.3 ± 0.1	8.9 ± 0.1
353.15	7.626	7.548	7.423	7.296	−0.24 ± 0.04	7.69 ± 0.04
358.15	6.757	6.682	6.570	6.455	−0.22 ± 0.04	6.81 ± 0.04
	Self-diffusion coefficient/10^{-10} m^2·s^{-1}				10^{-9} m^2·s^{-1}	10^{-10} m^2·s^{-1}
298.15	0.233	0.223	0.223	0.236	0.0 ± 0.1	0.228 ± 0.008
303.15	0.284	0.358	0.293	0.295	−0.1 ± 0.4	0.31 ± 0.04
308.15	0.356	0.358	0.363	0.362	0.1 ± 0.1	0.355 ± 0.001
313.15	0.452	0.451	0.465	0.446	0.0 ± 0.1	0.45 ± 0.01
318.15	0.552	0.549	0.572	0.550	0.1 ± 0.1	0.55 ± 0.01
323.15	0.670	0.672	0.727	0.668	0.2 ± 0.3	0.67 ± 0.03
328.15	0.851	0.826	0.820	0.799	−0.3 ± 0.1	0.855 ± 0.008
333.15	1.023	0.960	0.984	0.958	−0.4 ± 0.3	1.01 ± 0.03
338.15	1.121	1.130	1.163	1.145	0.3 ± 0.1	1.12 ± 0.01
343.15	1.293	1.323	1.301	1.312	0.1 ± 0.2	1.3 ± 0.02
348.15	1.467	1.510	1.628	1.611	1.3 ± 0.3	1.44 ± 0.03
353.15	1.848	1.723	1.725	1.759	−0.6 ± 0.5	1.82 ± 0.05
358.15	1.877	2.005	2.044	2.027	1.1 ± 0.4	1.89 ± 0.04

[a]Relative standard uncertainty of w and x_w is 0.05. Temperature standard uncertainty is estimated to be 0.02 K for the density and viscosity measurements and 0.3 K for the self-diffusion coefficient measurements. The shown standard deviations of the intercepts provide an estimate for the standard uncertainty of viscosity and self-diffusion coefficient, whereas for density, the relative standard uncertainty is limited by sample impurity to 0.001.

mole factions, x_w, are included in Tables 2−9 as well for convenience. Although we added approximately similar ranges of water up to mass fraction w = 0.02, the corresponding mole fractions increase from di- to nonaethylene glycol because of the increasing molar mass of the PEG oligomer. Figure 1 shows the trends in the data with respect to water mass fraction exemplary for 348.15 K. Density, viscosity, and self-diffusion coefficient in Figure 1 all display a linear relationship with water mass fraction. Therefore, we applied linear least squares fitting to find, for each water mass fraction-dependent dataset, the slope. The extrapolation to zero mass fraction (y- intercept) represents the property of the neat PEG. In this respect, we note that data values in Tables 2−9 are shown with more decimal places than the uncertainties stated in Section 2 for transparency and to

https://doi.org/10.1021/acs.jced.1c00101
J. Chem. Eng. Data 2021, 66, 2480−2500

Table 6. Density, Viscosity, and Self-Diffusion Coefficient of Hexaethylene Glycol with Small Amounts of Water in 10^{-6} Mass Fraction, w, as well as Mole Fraction, x_w, Present at Ambient Pressure (0.10 ± 0.01 MPa)[b]

	$w/10^{-6}$					
	5960	11,517	14,799	17,906		
	x_w					
T/K	0.086	0.154	0.191	0.222	slope[a]	intercept[a]
	Density/10^{-3} kg·m^{-3}				10^{-4} kg·m^{-3}	10^{-3} kg·m^{-3}
293.15	1.1264	1.1259	1.1197	1.1234	−2.5 ± 0.9	1.1282 ± 0.0012
298.15	1.1224	1.1220	1.1157	1.1194	−2.5 ± 1.0	1.1243 ± 0.0012
303.15	1.1183	1.1179	1.1117	1.1154	−2.5 ± 0.9	1.1201 ± 0.0012
308.15	1.1141	1.1138	1.1077	1.1115	−2.2 ± 0.9	1.1158 ± 0.0011
313.15	1.1100	1.1097	1.1036	1.1075	−2.1 ± 0.8	1.1116 ± 0.0011
318.15	1.1059	1.1056	1.0996	1.1035	−2.1 ± 0.8	1.1074 ± 0.0010
323.15	1.1019	1.1015	1.0955	1.0995	−2.0 ± 0.7	1.1034 ± 0.0009
328.15	1.0978	1.0974	1.0914	1.0954	−2.1 ± 0.8	1.0993 ± 0.0009
333.15	1.0937	1.0934	1.0874	1.0914	−2.0 ± 0.7	1.0951 ± 0.0009
338.15	1.0896	1.0893	1.0833	1.0873	−2.0 ± 0.7	1.0910 ± 0.0009
343.15	1.0856	1.0852	1.0792	1.0832	−2.0 ± 0.7	1.0871 ± 0.0009
348.15	1.0815	1.0811	1.0751	1.0792	−2.0 ± 0.6	1.0829 ± 0.0008
353.15	1.0774	1.0770	1.0711	1.0751	−2.0 ± 0.7	1.0788 ± 0.0008
358.15	1.0733	1.0729	1.0670	1.0710	−2.0 ± 0.7	1.0747 ± 0.0009
	Viscosity/mPa·s				10^2 mPa·s	mPa·s
293.15	84.105	83.435	79.580	81.841	−2.8 ± 2.0	86 ± 3.0
298.15	63.849	63.215	61.160	62.012	−1.9 ± 0.9	65 ± 1.2
303.15	49.377	48.949	47.410	47.767	−1.6 ± 0.6	50.4 ± 0.8
308.15	39.164	38.705	37.440	37.779	−1.4 ± 0.5	40.0 ± 0.7
313.15	31.467	31.118	30.090	30.442	−1.1 ± 0.4	32.1 ± 0.6
318.15	25.711	25.378	24.560	24.832	−0.9 ± 0.4	26.2 ± 0.5
323.15	21.303	21.012	20.430	20.661	−0.7 ± 0.3	21.7 ± 0.4
328.15	17.887	17.629	17.010	17.225	−0.7 ± 0.3	18.3 ± 0.4
333.15	15.130	14.919	14.280	14.474	−0.7 ± 0.3	15.5 ± 0.4
338.15	13.004	12.818	12.120	12.299	−0.7 ± 0.3	13.5 ± 0.4
343.15	11.365	11.192	10.420	10.551	−0.8 ± 0.3	11.9 ± 0.4
348.15	9.997	9.821	9.041	9.163	−0.8 ± 0.3	10.5 ± 0.4
353.15	8.659	8.513	7.938	8.026	−0.6 ± 0.2	9.1 ± 0.3
358.15	7.680	7.554	7.012	7.096	−0.6 ± 0.2	8.1 ± 0.3
	Self-diffusion coefficient/10^{-10} m^2·s^{-1}				10^{-9} m^2·s^{-1}	10^{-10} m^2·s^{-1}
298.15	0.195	0.182	0.185	0.192	−0.03 ± 0.08	0.19 ± 0.01
303.15	0.251	0.238	0.235	0.243	−0.1 ± 0.1	0.25 ± 0.01
308.15	0.315	0.310	0.296	0.309	−0.1 ± 0.1	0.32 ± 0.01
313.15	0.380	0.396	0.381	0.392	0.1 ± 0.1	0.38 ± 0.01
318.15	0.478	0.481	0.461	0.483	0.0 ± 0.1	0.48 ± 0.02
323.15	0.569	0.579	0.563	0.589	0.1 ± 0.1	0.56 ± 0.02
328.15	0.680	0.685	0.676	0.710	0.2 ± 0.2	0.66 ± 0.02
333.15	0.805	0.835	0.812	0.854	0.3 ± 0.2	0.79 ± 0.03
338.15	0.933	0.974	0.998	1.040	0.9 ± 0.1	0.88 ± 0.01
343.15	1.121	1.115	1.184	1.214	0.8 ± 0.3	1.05 ± 0.04
348.15	1.297	1.309	1.327	1.391	0.7 ± 0.3	1.24 ± 0.04
353.15	1.539	1.493	1.463	1.530	−0.2 ± 0.5	1.53 ± 0.06
358.15	1.797	1.727	1.802	1.821	0.3 ± 0.5	1.75 ± 0.07

[a]Slope and intercept values for density was obtained omitting the $w/10^{-6}$ = 14,799 data. [b]Relative standard uncertainty of w and x_w is 0.05. Temperature standard uncertainty is estimated to be 0.02 K for the density and viscosity measurements and 0.3 K for the self-diffusion coefficient measurements. The shown standard deviations of the intercepts provide an estimate for the standard uncertainty of viscosity and self-diffusion coefficient, whereas for density, the relative standard uncertainty is limited by sample impurity to 0.001.

eliminate rounding errors during fitting. The obtained slopes and extrapolated values for the neat PEG are included in Tables 2−9 and are shown with their standard deviations. We take these standard deviations as the standard uncertainty (68% confidence) of the neat PEG property.

Several specific observations should be noted, which are true for all temperatures (not shown). The slopes in Figure 1 are all negative for density and viscosity but positive for self-diffusion coefficient. This is, as expected, because the density and viscosity of water are lower than for the PEGs and self-diffusion coefficient is in inverse relation to viscosity. Next, there is a progressive increase in viscosity and a concurrent decrease in self-diffusion coefficient from di- to nonaethylene glycol. This is readily explained by the increased intermolecular interactions

https://doi.org/10.1021/acs.jced.1c00101
J. Chem. Eng. Data 2021, 66, 2480−2500

Table 7. Density, Viscosity, and Self-Diffusion Coefficient of Heptaethylene Glycol with Small Amounts of Water in 10^{-6} Mass Fraction, w, as well as Mole Fraction, x_w, Present at Ambient Pressure (0.10 ± 0.01 MPa)[a]

	$w/10^{-6}$					
	3457	5295	12,591	15,413		
	x_w					
T/K	0.059	0.088	0.188	0.221	slope	intercept
	Density/10^{-3} kg·m^{-3}				10^{-4} kg·m^{-3}	10^{-3} kg·m^{-3}
293.15	1.1251	1.1238	1.1222	1.1231	−1.8 ± 0.9	1.125 ± 0.001
298.15	1.1212	1.1197	1.1182	1.1190	−1.8 ± 0.9	1.121 ± 0.001
303.15	1.1172	1.1157	1.1141	1.1150	−1.9 ± 0.9	1.117 ± 0.001
308.15	1.1132	1.1116	1.1101	1.1109	−1.9 ± 0.9	1.113 ± 0.001
313.15	1.1092	1.1076	1.1061	1.1068	−2.0 ± 0.9	1.109 ± 0.001
318.15	1.1052	1.1036	1.1021	1.1028	−2.0 ± 0.9	1.105 ± 0.001
323.15	1.1013	1.0996	1.0977	1.0987	−2.2 ± 1.1	1.101 ± 0.001
328.15	1.0972	1.0955	1.0937	1.0946	−2.2 ± 1.0	1.097 ± 0.001
333.15	1.0932	1.0915	1.0897	1.0906	−2.2 ± 1.0	1.093 ± 0.001
338.15	1.0891	1.0874	1.0857	1.0865	−2.1 ± 1.0	1.089 ± 0.001
343.15	1.0851	1.0833	1.0817	1.0824	−2.2 ± 1.0	1.085 ± 0.001
348.15	1.0810	1.0793	1.0777	1.0783	−2.2 ± 0.9	1.081 ± 0.001
353.15	1.0769	1.0752	1.0734	1.0742	−2.2 ± 1.0	1.077 ± 0.001
358.15	1.0728	1.0711	1.0695	1.0700	−2.2 ± 0.9	1.073 ± 0.001
	Viscosity/mPa·s				10^2 mPa·s	mPa·s
293.15	97.270	93.780	92.260	92.020	−3.7 ± 1.5	97.2 ± 1.5
298.15	73.660	71.340	69.660	69.890	−2.9 ± 1.0	73.8 ± 1.1
303.15	57.030	53.690	53.760	53.680	−1.9 ± 1.5	56.3 ± 1.6
308.15	45.140	42.570	42.350	42.290	−1.8 ± 1.2	44.7 ± 1.2
313.15	36.260	34.290	33.980	33.970	−1.5 ± 0.9	36.0 ± 0.9
318.15	29.640	28.000	27.720	27.670	−1.3 ± 0.7	29.4 ± 0.8
323.15	24.530	23.210	22.880	22.860	−1.1 ± 0.6	24.4 ± 0.6
328.15	20.650	19.580	19.230	19.230	−1.0 ± 0.5	20.6 ± 0.5
333.15	17.420	16.500	16.170	16.150	−0.9 ± 0.4	17.4 ± 0.4
338.15	14.810	14.010	13.730	13.710	−0.8 ± 0.3	14.8 ± 0.4
343.15	12.690	12.030	11.750	11.740	−0.7 ± 0.3	12.7 ± 0.3
348.15	10.980	10.410	10.180	10.170	−0.6 ± 0.2	11.0 ± 0.3
353.15	9.587	9.103	8.903	8.870	−0.5 ± 0.2	9.6 ± 0.2
358.15	8.444	8.019	7.871	7.828	−0.4 ± 0.2	8.4 ± 0.2
	Self-diffusion coefficient/10^{-10} m^2·s^{-1}				10^{-9} m^2·s^{-1}	10^{-10} m^2·s^{-1}
298.15	0.160	0.155	0.166	0.155	0 ± 0.1	0.16 ± 0.01
303.15	0.206	0.197	0.220	0.191	0 ± 0.2	0.2 ± 0.02
308.15	0.257	0.259	0.276	0.272	0.16 ± 0.04	0.252 ± 0.005
313.15	0.336	0.327	0.351	0.336	0.1 ± 0.1	0.33 ± 0.01
318.15	0.422	0.403	0.372	0.509	0.5 ± 0.7	0.39 ± 0.07
323.15	0.485	0.479	0.536	0.510	0.4 ± 0.2	0.47 ± 0.02
328.15	0.585	0.588	0.631	0.621	0.4 ± 0.1	0.57 ± 0.01
333.15	0.676	0.691	0.792	0.738	0.7 ± 0.4	0.66 ± 0.04
338.15	0.810	0.817	0.871	0.834	0.3 ± 0.2	0.8 ± 0.03
343.15	0.958	0.962	1.051	1.016	0.7 ± 0.3	0.93 ± 0.03
348.15	1.109	1.107	1.128	1.135	0.24 ± 0.03	1.098 ± 0.003
353.15	1.285	1.233	1.315	1.378	0.9 ± 0.4	1.22 ± 0.04
358.15	1.493	1.454	1.578	1.612	1.2 ± 0.3	1.42 ± 0.03

[a]Relative standard uncertainty of w and x_w is 0.05. Temperature standard uncertainty is estimated to be 0.02 K for the density and viscosity measurements and 0.3 K for the self-diffusion coefficient measurements. The shown standard deviations of the intercepts provide an estimate for the standard uncertainty of viscosity and self-diffusion coefficient, whereas for density, the relative standard uncertainty is limited by sample impurity to 0.001.

between PEG molecules with increasing number of ethyleneoxide repeat units and associated increased molar mass.

The densities of di- to nonatheylene glycol in Figure 1 are overall within a narrow range of values, between 1076.7 kg·m^{-3} for diethylene glycol and 1082.9 for kg·m^{-3} for hexa- and nonaethylene glycol. There is no clear trend of neat densities from di- to nonaethylene glycol. The densities (y intercepts) of neat tri-, penta-, hepta-, and octaethylene glycol are all nearly identical, yet their slopes with respect to water content dependence vary noticeably. Within measurement uncertainties, the water content dependence of the densities for hexa- and nonaethylene glycol are essentially indistinguishable. We note that agreement with literature data as further described in

https://doi.org/10.1021/acs.jced.1c00101
J. Chem. Eng. Data 2021, 66, 2480−2500

Table 8. Density, Viscosity, and Self-Diffusion Coefficient of Octaethylene Glycol with Small Amounts of Water in 10^{-6} Mass Fraction, w, as well as Mole Fraction, x_w, Present at Ambient Pressure (0.10 ± 0.01 MPa)[a]

	$w/10^{-6}$					
	2141	6044	17,438	19,863		
	x_w					
T/K	0.042	0.111	0.267	0.294	slope	intercept
	Density/10^{-3} kg·m^{-3}				10^{-4} kg·m^{-3}	10^{-3} kg·m^{-3}
293.15	1.1253	1.1247	1.1228	1.1232	−1.3 ± 0.2	1.1255 ± 0.0003
298.15	1.1213	1.1206	1.1188	1.1191	−1.4 ± 0.2	1.1215 ± 0.0003
303.15	1.1173	1.1165	1.1148	1.1150	−1.4 ± 0.2	1.1175 ± 0.0003
308.15	1.1132	1.1125	1.1110	1.1110	−1.3 ± 0.1	1.1134 ± 0.0002
313.15	1.1092	1.1084	1.1071	1.1069	−1.3 ± 0.1	1.1093 ± 0.0002
318.15	1.1051	1.1044	1.1028	1.1029	−1.3 ± 0.2	1.1053 ± 0.0002
323.15	1.1011	1.1003	1.0989	1.0988	−1.3 ± 0.1	1.1012 ± 0.0002
328.15	1.0970	1.0962	1.0949	1.0947	−1.3 ± 0.1	1.0971 ± 0.0002
333.15	1.0930	1.0922	1.0909	1.0906	−1.3 ± 0.1	1.0931 ± 0.0001
338.15	1.0889	1.0881	1.0869	1.0866	−1.2 ± 0.1	1.0890 ± 0.0001
343.15	1.0849	1.0840	1.0828	1.0825	−1.3 ± 0.1	1.0850 ± 0.0002
348.15	1.0808	1.0800	1.0787	1.0784	−1.3 ± 0.1	1.0809 ± 0.0001
353.15	1.0768	1.0759	1.0746	1.0743	−1.3 ± 0.1	1.0769 ± 0.0002
358.15	1.0727	1.0718	1.0705	1.0702	−1.3 ± 0.1	1.0728 ± 0.0002
	Viscosity/mPa·s				10^2 mPa·s	mPa·s
293.15	108.40	107.41	102.99	98.404	−5.1 ± 1.2	110 ± 1.6
298.15	81.838	81.016	77.636	74.459	−3.8 ± 0.8	83.0 ± 1.1
303.15	63.333	62.629	60.339	57.332	−2.9 ± 0.8	64.2 ± 1.1
308.15	50.047	49.382	47.505	45.145	−2.4 ± 0.6	50.8 ± 0.8
313.15	40.202	39.670	38.033	36.191	−2.0 ± 0.5	40.8 ± 0.6
318.15	32.830	32.324	30.970	29.499	−1.7 ± 0.4	33.3 ± 0.5
323.15	27.172	26.736	25.551	24.362	−1.4 ± 0.3	27.6 ± 0.4
328.15	22.776	22.347	21.382	20.457	−1.2 ± 0.2	23.1 ± 0.3
333.15	19.289	18.974	18.131	17.247	−1.0 ± 0.2	19.6 ± 0.3
338.15	16.473	16.147	15.392	14.616	−0.9 ± 0.2	16.7 ± 0.3
343.15	14.152	13.850	13.188	12.530	−0.8 ± 0.2	14.4 ± 0.2
348.15	12.263	11.992	11.400	10.839	−0.7 ± 0.1	12.4 ± 0.2
353.15	10.718	10.468	9.954	9.457	−0.6 ± 0.1	10.9 ± 0.2
358.15	9.442	9.214	8.743	8.338	−0.6 ± 0.1	9.6 ± 0.1
	Self-diffusion Coefficient/10^{-10} m^2·s^{-1}				10^{-9} m^2·s^{-1}	10^{-10} m^2·s^{-1}
298.15	0.137	0.129	0.137	0.138	0.02 ± 0.03	0.132 ± 0.004
303.15	0.173	0.178	0.193	0.186	0.09 ± 0.03	0.172 ± 0.005
308.15	0.226	0.208	0.231	0.233	0.08 ± 0.07	0.215 ± 0.01
313.15	0.280	0.282	0.282	0.255	−0.1 ± 0.1	0.29 ± 0.01
318.15	0.357	0.386	0.343	0.413	0.1 ± 0.2	0.36 ± 0.03
323.15	0.420	0.437	0.445	0.439	0.1 ± 0.1	0.42 ± 0.01
328.15	0.509	0.521	0.539	0.539	0.17 ± 0.02	0.508 ± 0.003
333.15	0.602	0.612	0.696	0.632	0.3 ± 0.2	0.6 ± 0.03
338.15	0.718	0.706	0.778	0.725	0.2 ± 0.2	0.71 ± 0.03
343.15	0.852	0.834	0.873	0.847	0.1 ± 0.1	0.84 ± 0.02
348.15	0.980	0.984	1.062	1.021	0.4 ± 0.2	0.97 ± 0.02
353.15	1.079	1.112	1.205	1.202	0.7 ± 0.1	1.07 ± 0.01
358.15	1.287	1.344	1.296	1.447	0.5 ± 0.5	1.29 ± 0.07

[a]Relative standard uncertainty of w and x_w is 0.05. Temperature standard uncertainty is estimated to be 0.02 K for the density and viscosity measurements and 0.3 K for the self-diffusion coefficient measurements. The shown standard deviations of the intercepts provide an estimate for the standard uncertainty of viscosity and self-diffusion coefficient, whereas for density, the relative standard uncertainty is limited by sample impurity to 0.001.

Section 3.2 suggests that these trends are not due to inaccurate measurements.

The slopes of the least linear square fits for the density data in Figure 1 are varying erratically between di- to nonaethylene glycol, while the slopes for viscosity and self-diffusion in Figure 1 vary mostly due to random error the data sets. In this respect, data scatter is, for unknown reasons, larger for the density and viscosity data of hexaethylene glycol. We omitted the data points near 0.015 mass fraction for fitting the density data of hexaethylene glycol (see Figure 1a), which are outlying most likely due to the inadvertent presence of a small air bubble in the vibrating tube during measurement, which leads to inaccurate lower density values. We note that the viscosity and self-

https://doi.org/10.1021/acs.jced.1c00101
J. Chem. Eng. Data 2021, 66, 2480−2500

Table 9. Density, Viscosity, and Self-Diffusion Coefficient of Nonaethylene Glycol with Small Amounts of Water in 10^{-6} Mass Fraction, w, as well as Mole Fraction, x_w, Present at Ambient Pressure (0.10 ± 0.01 MPa)[a]

	$w/10^{-6}$					
	4413	5894	9903	14,712		
	x_w					
T/K	0.093	0.120	0.187	0.256	slope	intercept
	Density/10^{-3} kg·m^{-3}				10^{-4} kg·m^{-3}	10^{-3} kg·m^{-3}
293.15	1.1264	1.1262	1.1252	1.1238	−2.6 ± 0.2	1.1276 ± 0.0002
298.15	1.1223	1.1222	1.1213	1.1197	−2.6 ± 0.3	1.1236 ± 0.0003
303.15	1.1182	1.1182	1.1173	1.1157	−2.5 ± 0.3	1.1195 ± 0.0003
308.15	1.1141	1.1141	1.1133	1.1117	−2.4 ± 0.4	1.1154 ± 0.0004
313.15	1.1101	1.1101	1.1093	1.1078	−2.3 ± 0.3	1.1113 ± 0.0003
318.15	1.1061	1.1060	1.1053	1.1038	−2.3 ± 0.3	1.1073 ± 0.0003
323.15	1.1020	1.1020	1.1013	1.0999	−2.1 ± 0.3	1.1031 ± 0.0003
328.15	1.0980	1.0979	1.0972	1.0959	−2.1 ± 0.2	1.0991 ± 0.0002
333.15	1.0940	1.0939	1.0931	1.0920	−2.0 ± 0.2	1.0950 ± 0.0001
338.15	1.0900	1.0898	1.0891	1.0881	−1.9 ± 0.1	1.0909 ± 0.0001
343.15	1.0860	1.0857	1.0850	1.0841	−1.83 ± 0.02	1.08680 ± 0.00002
348.15	1.0820	1.0817	1.0809	1.0800	−1.94 ± 0.02	1.08285 ± 0.00002
353.15	1.0780	1.0777	1.0769	1.0759	−2.04 ± 0.01	1.07890 ± 0.00001
358.15	1.0740	1.0736	1.0728	1.0718	−2.1 ± 0.1	1.0749 ± 0.0001
	Viscosity/mPa·s				10^2 mPa·s	mPa·s
293.15	124.50	121.55	120.74	117.40	−6.0 ± 1.4	126.3 ± 1.3
298.15	93.986	92.081	91.487	88.732	−4.5 ± 0.9	95.5 ± 0.9
303.15	72.590	71.175	70.109	68.336	−3.8 ± 0.5	73.9 ± 0.5
308.15	57.450	56.400	55.245	54.277	−2.9 ± 0.5	58.4 ± 0.5
313.15	46.045	45.219	44.271	43.466	−2.4 ± 0.4	46.8 ± 0.4
318.15	37.506	36.830	36.030	35.362	−2.0 ± 0.3	38.2 ± 0.3
323.15	30.968	30.409	29.761	29.189	−1.6 ± 0.2	31.5 ± 0.2
328.15	25.913	25.444	24.905	24.402	−1.4 ± 0.2	26.4 ± 0.2
333.15	21.920	21.514	21.061	20.849	−1.0 ± 0.2	22.2 ± 0.2
338.15	18.760	18.443	18.092	17.653	−1.0 ± 0.1	19.1 ± 0.1
343.15	16.155	15.829	15.469	15.067	−1.0 ± 0.1	16.5 ± 0.1
348.15	13.999	13.684	13.353	12.964	−0.9 ± 0.1	14.3 ± 0.1
353.15	12.206	11.928	11.617	11.279	−0.9 ± 0.1	12.5 ± 0.1
358.15	10.721	10.473	10.206	9.897	−0.8 ± 0.1	11.0 ± 0.1
	Self-Diffusion Coefficient/10^{-10} m^2·s^{-1}				10^{-9} m^2·s^{-1}	10^{-10} m^2·s^{-1}
298.15	0.109	0.121	0.128	0.118	0.1 ± 0.1	0.11 ± 0.01
303.15	0.146	0.151	0.172	0.163	0.2 ± 0.1	0.14 ± 0.01
308.15	0.195	0.214	0.216	0.201	0.0 ± 0.2	0.21 ± 0.02
313.15	0.261	0.248	0.278	0.267	0.1 ± 0.2	0.25 ± 0.02
318.15	0.294	0.310	0.332	0.313	0.2 ± 0.2	0.30 ± 0.02
323.15	0.355	0.382	0.387	0.387	0.2 ± 0.2	0.36 ± 0.02
328.15	0.429	0.467	0.449	0.462	0.2 ± 0.2	0.44 ± 0.02
333.15	0.516	0.544	0.544	0.548	0.2 ± 0.2	0.52 ± 0.02
338.15	0.597	0.633	0.640	0.660	0.5 ± 0.2	0.59 ± 0.02
343.15	0.705	0.731	0.777	0.762	0.6 ± 0.3	0.70 ± 0.03
348.15	0.815	0.823	0.840	0.885	0.7 ± 0.1	0.78 ± 0.01
353.15	0.922	0.981	1.020	1.010	0.7 ± 0.4	0.92 ± 0.04
358.15	1.091	1.157	1.143	1.194	0.8 ± 0.4	1.08 ± 0.03

[a]Relative standard uncertainty of w and x_w is 0.05. Temperature standard uncertainty is estimated to be 0.02 K for the density and viscosity measurements and 0.3 K for the self-diffusion coefficient measurements. The shown standard deviations of the intercepts provide an estimate for the standard uncertainty of viscosity and self-diffusion coefficient, whereas for density, the relative standard uncertainty is limited by sample impurity to 0.001.

diffusion coefficient measurements of this same sample showed no indication of inaccuracy.

The PEG oligomers and water can both act as hydrogen bond donors and acceptors. Water added to a PEG oligomer is competing as hydrogen bond partner between the inter- and intramolecular hydrogen bonding interactions present in the native PEG oligomer. The interplay of these hydrogen bonding interactions (along with other molecular interactions) should impact the configurational structure of PEG and thus the material properties of these water PEG oligomer mixtures. For example, molecular dynamics (MD) simulations of PEG as a solute in water and other solvents[149,150] show that PEG tends to take on a helical configuration in water, while other configurations are observed in less polar solvents. Thus, it is

https://doi.org/10.1021/acs.jced.1c00101
J. Chem. Eng. Data 2021, 66, 2480−2500

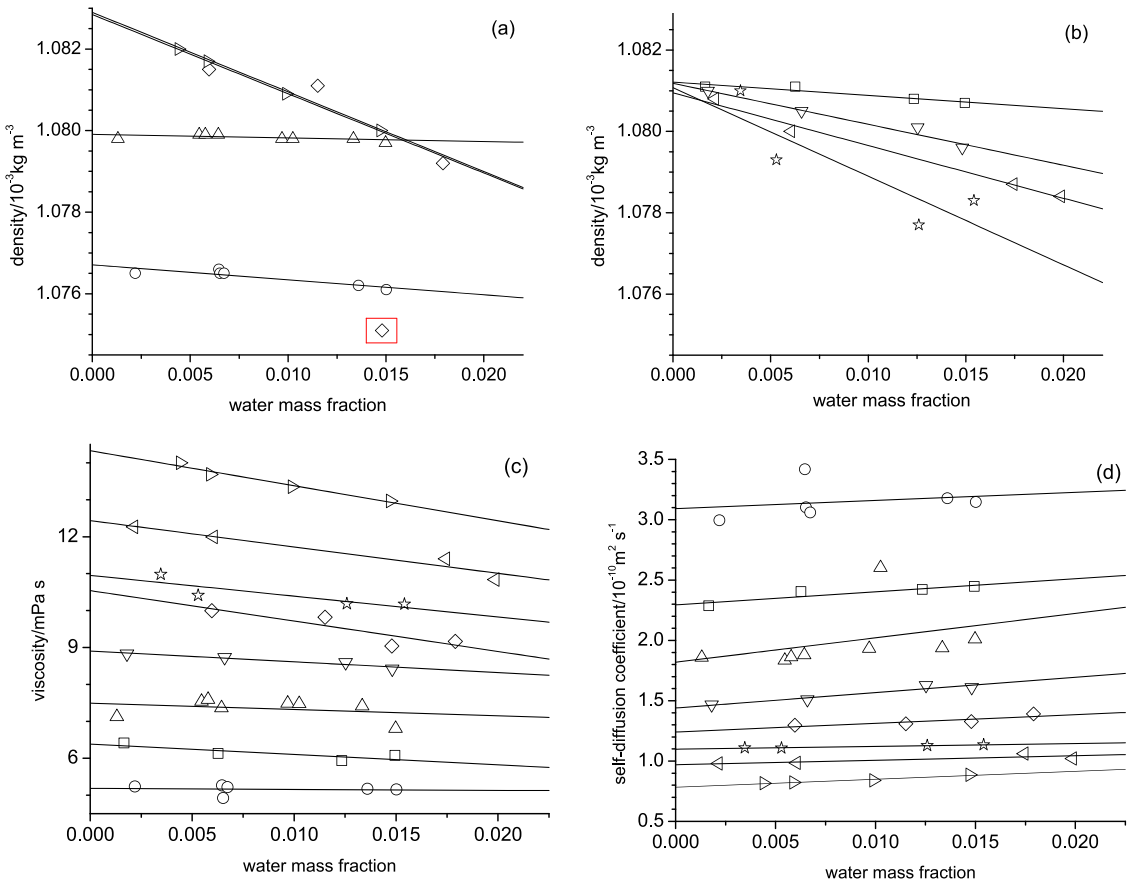

Figure 1. Density (a, b), viscosity (c), and self-diffusion coefficient (d) of diethylene glycol (circles), triethylene glycol (squares), tetraethylene glycol (triangles), pentaethylene glycol (inverted triangles), hexaethylene glycol (diamonds), heptaethylene glycol (stars), octaethylene glycol (left-pointing triangles), and nonaethylene glycol (right-pointing triangles) as a function of mass fraction at 348.15 K. The solid lines are linear least squares lines. The red square highlights an outlying data point not included in the linear fitting.

perhaps surprising that the effect of water on density, viscosity, and self-diffusion coefficient is not more pronounced as observed in Figure 1. Thus, beyond the scope of this report, MD simulations of PEG oligomers with small amounts of present water are underway to help develop a molecular-level understanding on the influence of the added water on the liquid structure of the PEG oligomers. The findings from these ongoing MD simulations will be reported in due course.

3.2. Comparison with the Literature. There are substantial amounts of literature data for the densities and viscosities of the smaller PEG oligomers. Tables 10 and 11 present percent relative deviations, %RD = (value$_{\text{this study}}$ − value$_{\text{literature}}$)/value$_{\text{this study}}$, of these literature values to our density and viscosity results, respectively, for literature data sets containing four or less entries. Comparisons of our results with literature data sets containing more than four data points are shown graphically for di-, tri-, and tetraethylene glycol, respectively, in Figures 2−4 for density and Figures 5−7 for viscosity. Values for %RD were obtained for data from temperatures that do not match temperatures of our data sets by interpolation. Overall, nearly all of the density literature data sets are in agreement with the results in this report within 0.2%. For the viscosity, agreement is within 10% for the majority of the literature values.

One general observation that can be made in Tables 10 and 11 and Figures 2−7 is that the %RDs tend to be negative, which means our reported results tend to be larger compared to most literature data. Principally, this could indicate the effect of water impurity present that, through our extrapolation methods, we more carefully accounted for. As we have shown in Section 3.1, the presence of water slightly decreases both density and viscosity of the studied PEG oligomers. However, the %RDs in the density data, which majorly lie between 0.05 and 0.1, are larger than what could be accounted for from the effect of present water based on the graphs in Figure 1. Interestingly, the careful study by Carvalho et al.[100] reports two density data sets (included in Figures 2−4) independently measured with two different instruments, and our results lie between these two data sets, except for tetraetheylene glycol (Figure 4) where our data nearly overlap with their lower density data set. We note in this regard that only few studies even have reported the PEG water content.[86,92,101,136,151] We also note that most literature data sets (Figures 2−4) show constant %RD with temperature relative to our results. This indicates that temperature errors such as calibration or equilibration are not a significant source of measurement error in these and our data sets. Conversely, temperature-related errors might be indicated for those data sets that do not show a constant %RD with temperature in Figures 2−4.

As for comparing our viscosity results with literature data sets, values for %RD in Table 11 and Figures 5−7 are much larger compared to density data sets for same samples at the same experimental temperature conditions. This is understandable in light of a much stronger, exponential temperature dependence (see Section 3.3) and a larger standard uncertainty achievable compared to density measurements. That said, in Figures 5−6,

https://doi.org/10.1021/acs.jced.1c00101
J. Chem. Eng. Data 2021, 66, 2480−2500

Table 10. % Relative Deviations of Literature Data to Density Measurements in This Work

	diethylene glycol				
293.15 K	−0.13[96]	−0.08[104−107]	−0.14[117]		
298.15 K	−0.09[87]	−0.004[91]	−0.012[93]	−0.09[95]	−0.04[96]
	−0.11[97]	−0.06[104−107]	−0.11[110]	−0.02[112]	−0.012[114,115]
	−0.06[118]				
303.15 K	−0.07[87]	−0.04[96,114,115]	−0.02[97]	−0.06[102,103,130,131]	−0.05[104−107,116]
	0.20[61]				
308.15 K	−0.05[87,110]	−0.04[96]	−0.07[97]	−0.017[114,115]	−0.08[58,59]
	−0.02[116]	−0.06[118]			
313.15 K	−0.02[87]	−0.04[97]	−0.02[114,115]	−0.12[117]	
318.15 K	−0.05[118]				
328.15 K	−0.04[118]				
333.15 K	−0.05[117]				
	triethylene glycol				
293.15 K	−0.09[96]	−0.06[104−107]	−0.10[117]		
298.15 K	−0.09[95,96,115,139]	−0.08[104−107]	−0.07[110]	−0.06[118]	
303.15 K	−0.09[96,114,130,131]	−0.05[102]	−0.08[104−107]	−0.07[114,115]	−0.03[116]
308.15 K	−0.09[96]	−0.02[110]	−0.014[112]	−0.07[114,115]	−0.06[58,59,118]
	−0.008[116]				
313.14 K	−0.16[135]				
313.15 K	−0.06[114,115]	−0.08[117]			
318.15 K	−0.06[118]				
328.15 K	−0.06[118]				
333.15 K	−0.06[117]				
348.13 K	−0.14[135]				
	tetraethylene glycol				
293.15 K	−0.04[104−107]	−0.07[117]			
298.15 K	−0.013[95]	0.02[104−107]	0.013[109]	0.09[112]	0.03[118]
303.15 K	0.04[130,131]	0.09[104−107,116]			
308.15 K	0.03[110,118]	0.10[116]			
313.15 K	−0.07[117]				
318.15 K	0.002[118]				
328.15 K	0.03[118]				
333.15 K	−0.07[117]				
	hexaethylene glycol				
333.15 K	−0.03[141]				

there are clearly some data sets that are exceedingly in disagreement (%RD > 10) with the majority of the other data sets. Specifically, for diethylene glycol in Figure 5, the data set of Li et al.[88] deviates by more than −10%, the data set by Kumagai et al.[117] up to −22%, and the data set by Wang et al.[89] deviates by about −40%. For triethylene glycol in Figure 6, the data set by Chen et al.[138] stands out with %RDs increasing with temperature from about −20 to about −45. The data sets by Sagdeev et al.[108,109] for diethylene glycol in Figure 5 and Hao et al.[127] and Qiao et al.[128] for triethylene glycol in Figure 6 appear to include one erroneous outlying data point. Single point measurements for triethylene glycol by Farag et al.[140] (−16% deviation) as well as by Pande and Kalamse[139] et al. (−35% deviation) in Table 11 are also in excessive disagreement. Some data sets in Figures 5−7 show increasing %RD with increasing temperature. This may not necessarily be an error in temperature calibration or equilibration, but due to an offset in their viscosity calibration. For example, a deviation of 0.5 mPa·s is a smaller %RD at 298.15 K because at 338.15 K the viscosity is of a larger value. Overall, agreement of our viscosity data with the literature is generally within a few percent.

We conclude this sub-section by reiterating our statement in Section 1 that we are unaware of literature data for self-diffusion coefficients for the neat PEG oligomers studied here.

3.3. Temperature Dependence. Figure 8 shows exemplarily the density as a function of temperature for di- and nonaethylene glycol. A linear temperature dependence of the density is evident from Figure 8. Nevertheless, besides linear least squares fits, also fitting to second-order polynomials was carried out and the results and statistics are summarized in Table S3 in the Supporting Information. Indeed, the fitting coefficient for the square dependence is very small and does not consistently have the same sign across all PEG oligomers. This clearly shows that nonlinearity of the density temperature dependence is not indicated within uncertainty of the data, which is smaller than the size of the symbols in Figure 8.

The graphs in Figure 9 show the logarithmic plots of viscosity and self-diffusion coefficient against inverse temperature for several of the PEG oligomers. Nonlinearity of these plots indicates that temperature dependencies of these properties do not follow the Arrhenius law and should be fitted instead with the Vogel−Fulcher−Tammann (VFT) equation. Both relations are shown in logarithmic form in eqs 2 and 3, respectively:

https://doi.org/10.1021/acs.jced.1c00101
J. Chem. Eng. Data 2021, 66, 2480−2500

Table 11. % Relative Deviations of Literature Data to Viscosity Measurements in This Work

	diethylene glycol				
293.15 K	−0.3[96]	3.3[126]	7.8[120−123]	−6.7[117]	
294.2 K	−2.2[119]				
298. 15 K	0.5[91]	−4.3[93]	−1.3[96]	−3.1[97]	7.0[120−123]
	7.1[114,115]				
303.15 K	0.5[96]	−2.2[97,120−125]	−2.8[116]		
308.15 K	0.5[96]	−5.0[97]	−6.6[114,115]	−3.2[58,59]	−4.5[116]
313.05 K	−0.6[119]				
313.15 K	−15.4[117]	−2.1[97]			
333.05 K	−2.3[119]				
333.15 K	−22.7[117]				
	triethylene glycol				
293.15 K	1.3[96]	5.6[126]	−13.6[120−123]	−2.8[117]	
298.15 K	−0.6[96]	−0.8[108]	−7.3[114,115,120−123]	−35.3[139]	
299.65 K	1.1[119]				
303.15 K	1.4[96]	−16.4[140]	0.2[120−125]	0.3[116]	
308.15 K	1.3[96]	−9.0[114,115]	1.9[58,59]	−2.4[116]	
312.96 K	−1.4[108]				
313.05 K	1.5[119]				
313.15 K	−9.1[117]				
333.10 K	1.1[119]				
333.15 K	−4.7[117]				
334.96 K	−0.7[108]				
349.25 K	−3.9[108]				
353.05 K	0.7[119]				
	tetraethylene glycol				
293.15 K	3.6[126]	−9.9[120−123]	−2.8[117]		
298.15 K	−2.4[120−123]				
303.15 K	0.4[120−125]	−9,3[140]	−2.7[116]		
308.15 K	−4.8[116]				
313.15 K	−0.5[117]				
333.15 K	4.9[117]				
	pentaethylene glycol				
293.15 K	2.1[126]				
	hexaethylene glycol				
293.15 K	2.1[126]				
	heptaethylene glycol				
293.15 K	2.4[126]				

$$\ln(X(T)) = \ln A \pm \frac{E_a}{RT} \quad (2)$$

$$\ln(X(T)) = \ln y_0 \pm \frac{B}{(T - T_0)} \quad (3)$$

where $X(T)$ represents the temperature-dependent property and the sign before the second term of the right-hand equation is positive for viscosity and negative for self-diffusion coefficients. E_a and A and y_0, B, and T_0 are the material-dependent fit parameters for the Arrhenius and VFT equation, respectively. For the Arrhenius equation, E_a has the physical meaning of the activation energy and A is referred to as the pre-exponential factor. For the VFT equation, y_0 is also a pre-exponential factor, B represents the fragility strength coefficient, and T_0 is referred to as the Vogel divergence temperature, which should be below the glass transition temperature for glass-forming substances. Visual inspection of the graphs in Figure 9 indicates slight deviations from linearity over the investigated temperature ranges for both viscosity and self-diffusion coefficients. The fitting results to both eqs 2 and 3 are summarized in Table S4 in the Supporting Information. It can be observed that activation energies are in close agreement for viscosity and self-diffusion coefficients, indicating that the same underlying dynamics govern the process of momentum transfer and mass transport in these PEG oligomers. In contrast, the values for fit parameter B for the VFT equation are observed to differ by up to a factor 2 between viscosity and self-diffusion coefficient. This may indicate that a wider range of temperatures needs to be investigated to obtain more reliable fit parameters for the VFT equation to properly account for the deviations from the Arrhenius law. The trend of the activation energies with respect to the homologous series will be part of Section 3.4.

3.4. Homologous Series. We have already pointed out in Section 3.1 that densities are all rather similar between the oligomers and that there is no clear trend in their ordering with regard to the homologous series of the PEG oligomers. This is true also if one just inspects separately the PEG oligomers with even and odd numbered ethylene oxide repeat units. This is unfortunate because the consequence is that prediction of densities for PEG oligomers larger than nonaethylene glycol is not permissible. As best educated guess, one may presume that

https://doi.org/10.1021/acs.jced.1c00101
J. Chem. Eng. Data 2021, 66, 2480−2500

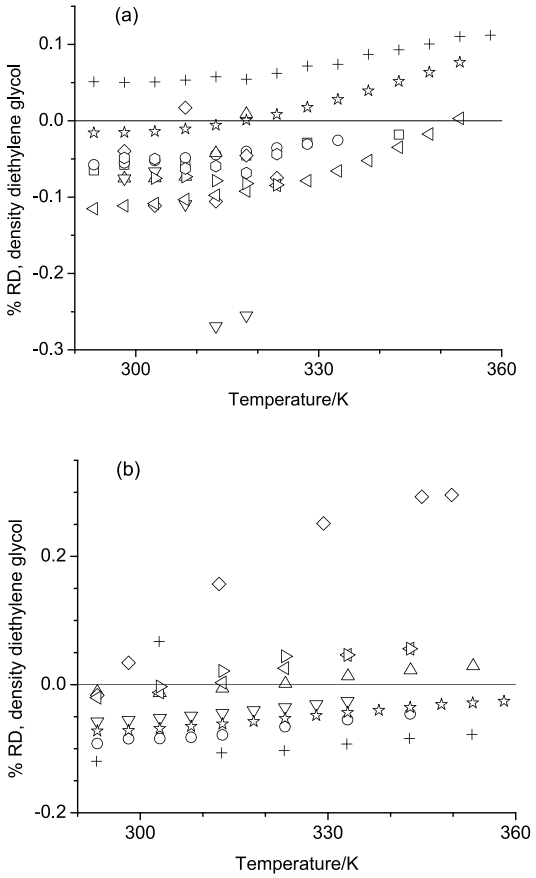

Figure 2. % Relative deviation (%RD) of diethylene glycol density of results from (a) Ghaedi et al.[25] (squares), Klimaszewkski et al.[86] (circles), Li et al.[88] (triangles), Wang et al.[89] (inverted triangles), Huo et al.[90] (diamonds), Cocchi et al.,[92] (left-pointing triangles), Ren et al.[94] (right-pointing triangles), Begum et al.[98] (hexagons), Bernal-García[99] (stars), and Carvalho et al.[100] (plus sign) and (b) Carvalho et al.[100] (circles), Crespo et al.[101] (triangles), Klimaszewkski et al.[86] (inverted triangles), Sagdeev et al.[108,109] (diamonds), Chen et al.[111] (left-pointing triangles), Mesquita et al.[113] (right-pointing triangles), Afzal et al.[60] (stars), and Pereira et al.[62] (plus sign) to the results of this study.

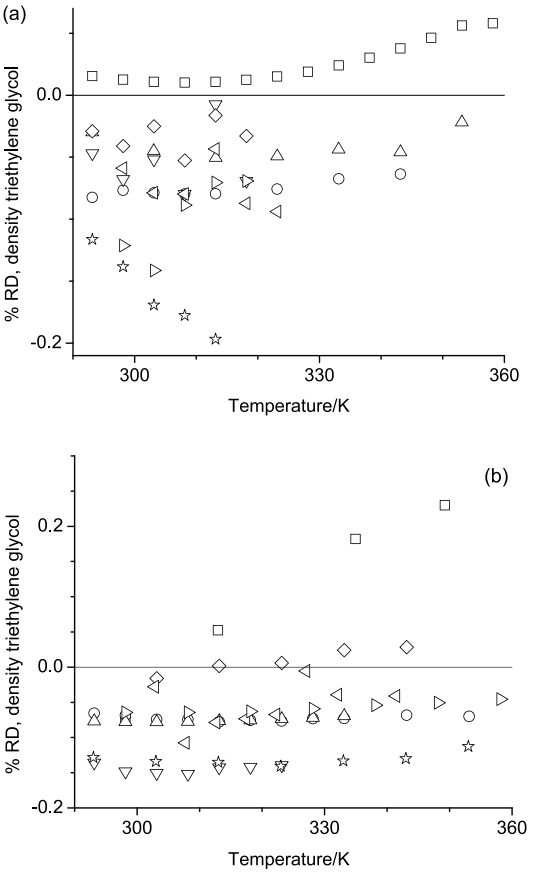

Figure 3. % Relative deviation (%RD) of triethylene glycol density of results from (a) Carvalho et al.[100] (squares), Carvalho et al.[100] (circles), Crespo et al.[101] (triangles), Hao et al.[127] (inverted triangles), Qiao et al.[128] (diamonds), Begum et al.[129] (left-pointing triangles), Guo et al.[132] (right-pointing triangles), and Aniya et al.[133] (stars) and (b) Sagdeev et al.[108,109] (squares), Valtz et al.[134] (circles), Klimaszewski et al.[136] (triangles), Almasi[137] (inverted triangles), Mesquita et al.[113] (diamonds), Chen et al.[138] (left-pointing triangles), Afzal et al.[60] (right-pointing triangles), and Pereira et al.[62] (stars) to the results of this study.

density will continue to stay relatively flat with increasing size of oligomer or, at best, only slightly increase.

The situation with respect to predicting physicochemical properties of higher homologies is more encouraging for the viscosity and self-diffusion coefficients. As can be seen in Figure 10, exemplarily for the data at 348.15 K, the natural log of viscosity as well as of self-diffusion coefficient appear to be smooth functions of the number of ethylene oxide repeat unit, n, which we fitted with second-order polynomials. The obtained fit coefficients and statistics are summarized in Tables S5 and S6 in the Supporting Information, respectively, for the viscosity and self-diffusion coefficients for the eight PEG oligomers studied.

Possibly, a more reliable approach to predict viscosities and self-diffusion coefficients of higher oligomers is based on the dependencies of the activation energies and pre-exponential factors with respect to the number of ethylene oxide repeat unit, n. As can be seen in Figure 11, the activation energies appear to be linearly dependent to n as shown in eq 4:

$$E_a/(\mathrm{kJ\cdot mol^{-1}}) = (0.456 \pm 0.050)n + (28.85 \pm 0.30) \quad (4)$$

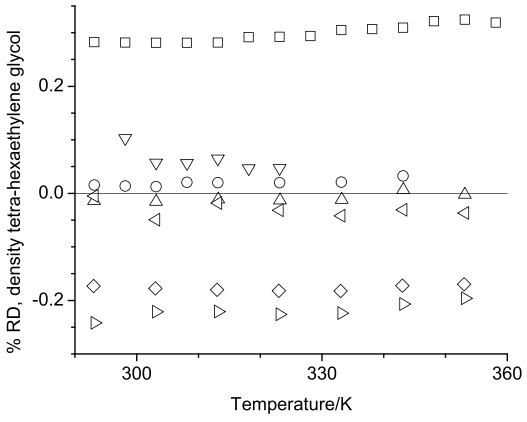

Figure 4. % Relative deviation (%RD) of tetraethylene glycol density results from Carvalho et al.[100] (squares), Carvalho et al.[100] (circles), Crespo et al.[101] (triangles), Begum et al.[129] (inverted triangles), Pereira et al.[62] (diamonds), as well as pentaethylene glycol (left-pointing triangles) and hexaethylene glycol (right-pointing triangles) density results from Crespo et al.[101] to the results of this study.

https://doi.org/10.1021/acs.jced.1c00101
J. Chem. Eng. Data 2021, 66, 2480−2500

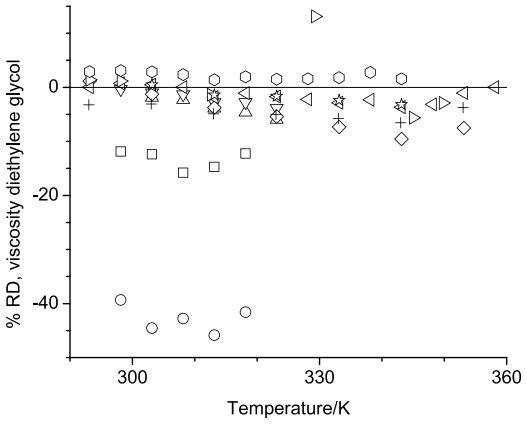

Figure 5. % Relative deviation (%RD) of diethylene glycol viscosity results from Li et al.[88] (squares), Wang et al.[89] (circles), Ren et al.[94] (triangles), Begum et al.[98] (inverted triangles), Bernal-Garća et al.[99] (diamonds), Carvalho et al.[100] (left-pointing triangles), Sagdeev et al.[108,109] (right-pointing triangles), Ghaedi et al.[23] (hexagons), Mesquita et al.[113] (stars), and Pereira et al.[62] (plus sign) to the results of this study.

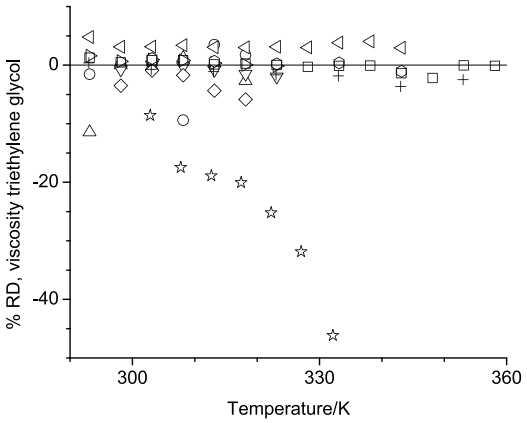

Figure 6. % Relative deviation (%RD) of triethylene glycol viscosity results from Carvalho et al.[100] (squares), Hao et al.[127] (circles), Qiao et al.[128] (triangles), Begum et al.[98] (inverted triangles), Guo et al.[132] (diamonds), Ghaedi et al.[23] (left-pointing triangles), Almasi[137] (right-pointing triangles), Mesquita et al.[113] (hexagons), Chen et al.[138] (stars), and Pereira et al.[62] (plus sign) to the results of this study.

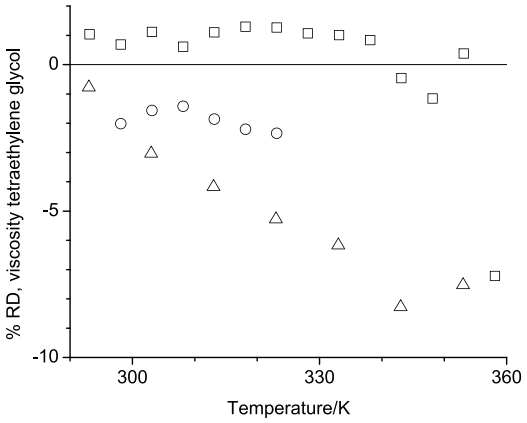

Figure 7. % Relative deviation (%RD) of tetraethylene glycol viscosity results from Carvalho et al.[100] (squares), Begum et al.[98] (circles), and Pereira et al.[62] (triangles) to the results of this study.

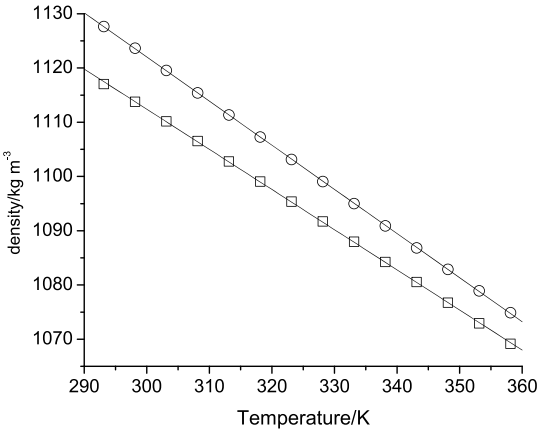

Figure 8. Temperature dependence of density for diethylene glycol (squares) and nonaethylene glycol (circles). The lines are from least squares linear line fits.

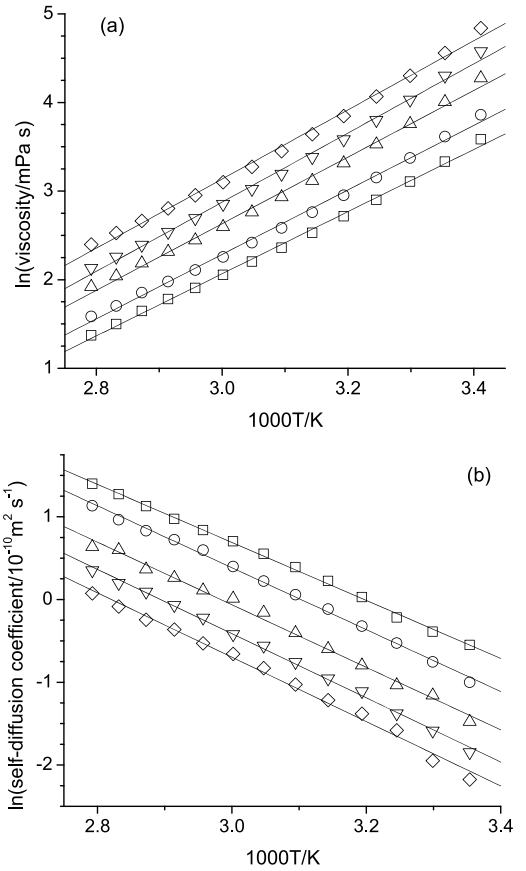

Figure 9. Arrhenius plots for the temperature dependence of (a) viscosity and (b) self-diffusion coefficient of diethylene glycol (squares), triethylene glycol (circles), pentaethylene glycol (triangles), heptaethylene glycol (inverted triangles), and nonaethylene glycol (diamonds). The lines are from least squares linear line fits.

which was obtained using the activation energies from both the viscosity and self-diffusion data since, as pointed out in Section 3.3, they are identical within experimental uncertainty. Equation 4 is shown as the solid line in Figure 11 and fits the data well within measurement uncertainty expect perhaps for diethylene glycol. Additional data from higher liquid PEG oligomers would be desirable to confirm the linearity invoked in eq 4. Assuming that eq 4 is principally valid, we next inspect the pre-exponential

https://doi.org/10.1021/acs.jced.1c00101
J. Chem. Eng. Data 2021, 66, 2480−2500

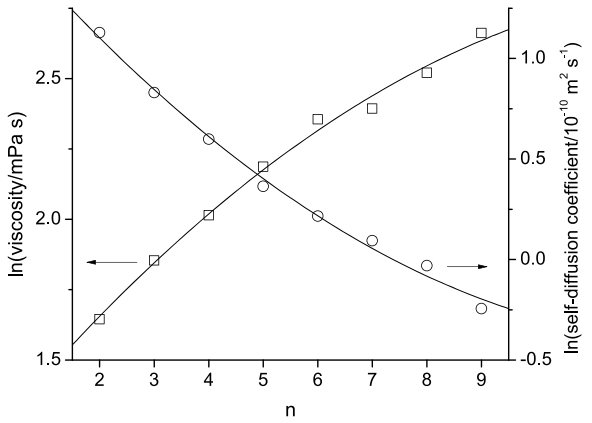

Figure 10. Inspection of homologous series of polyethylene glycol oligomers for the natural logarithm of viscosity (squares) and self-diffusion coefficient (circles) at 348.15 K as a function of ethylene oxide repeat units. The solid lines are second-order polynomial fits.

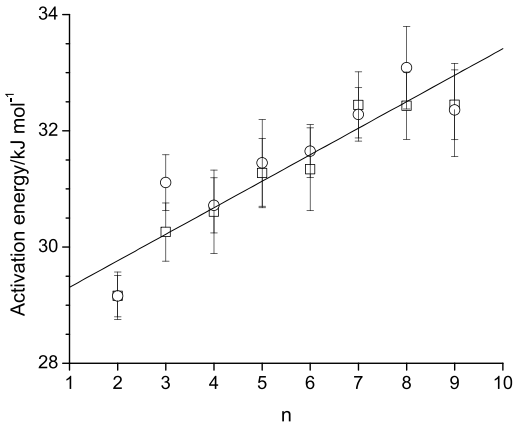

Figure 11. Activation energies from viscosities (squares) and self-diffusion coefficients (circles) as a function ethylene oxide repeat units of PEG oligomers. The solid line is from a least squares linear line fit.

factors. From Table S4 in the Supporting Information, it can be seen that they are essentially independent of n. Averages of the pre-exponential factor result in $\ln(A/\text{mPa·s}) = -8.62 \pm 0.12$ for the viscosity data and $\ln(A/10^{-10}\ \text{m}^2\text{·s}^{-1}) = 11.27 \pm 0.18$ for the self-diffusion data. Thus, these averages in combination with eq 4 may be used to estimate the viscosity or self-diffusion coefficient of neat oligomers with $n > 9$ for the temperature range investigated in this study.

We also inspected for homologous series trends with regard to the ratio of $(k_B T)/(\pi\eta D)$, which, according to the Stokes–Einstein, eq 5, should be approximately constant as it relates to the hydrodynamic radius, r, of, in this case, the PEG oligomer.

$$r = \frac{k_B T}{c\pi\eta D} \tag{5}$$

In eq 5, k_B is the Boltzmann constant, η is the viscosity, D is the self-diffusion coefficient, and c is a constant typically ranging between 4 and 6 for the slip and stick boundary conditions.[152]

The evaluations with standard uncertainties obtained through error propagation are summarized in Table S7 in the Supporting Information. The values are, as expected, increasing with oligomer size. They are also increasing with temperature by about 10% from 298.15 to 358.15 K, which indicates that c is changing with temperature. The dependence of $(k_B T)/(\pi\eta D)$ as a function of the number of ethylene oxide repeat units could be fitted reasonably well with second-order polynomials (not shown). However, present data scatter and uncertainties appear to make this approach to estimate viscosities and self-diffusion coefficients of higher PEG oligomers not more promising than using the above described approach of the Arrhenius equation along with eq 4 and the listed average values for the pre-exponential factors.

4. CONCLUSIONS

New data on density, viscosity, and self-diffusion coefficient for oligomers of PEG from di- to nonaethylene glycol over a wide range of temperatures were presented. To take into account water as the most common impurity in PEGs, the results were obtained by extrapolation from measurements as a function of present water. The effect of the presence of water was found to be small but systematically lowering the density and viscosity and increasing the self-diffusion coefficient. Neglecting the effect of present water could be a contributing factor that densities and viscosities reported here were generally higher than most reported in the literature as only few even have reported the PEG water content.[86,92,101,136,151] A linear temperature dependence was found for the densities over the investigated temperature range. With caution, this allows extrapolation to obtain reasonable estimates for densities outside the temperature range measured in this study. As for viscosity and self-diffusion coefficient, additional data over a wider range of temperatures is needed to more accurately capture the non-linearity in the Arrhenius graphs. Nevertheless, the obtained activation energies from the Arrhenius analysis appear to be the same for viscosity and self-diffusion coefficients. Moreover, the pre-exponential factors for viscosity and self-diffusion coefficients each appeared to be identical for the eight studied oligomers while the activation energies appear to be linearly dependent on the number of ethylene oxide repeat units in the PEG oligomer. This may serve as an approach for estimating viscosities and self-diffusion coefficients for higher oligomers. The densities of the oligomers are all within a rather narrow range at a given temperature but otherwise do not show any systematic trend in the homologous series. Overall, this study has extended considerably the available physicochemical property data of PEG oligomers. To the best of our knowledge, these are the first reported measurements for self-diffusion coefficients for all of the studied PEG oligomers as well as the first temperature-dependent density measurements for hepta- to nonaethylene glycol and temperature-dependent viscosity measurements for penta- to nonaethylene glycol.

■ ASSOCIATED CONTENT

Supporting Information

The Supporting Information is available free of charge at https://pubs.acs.org/doi/10.1021/acs.jced.1c00101.

Tables with standard deviations for viscosity and self-diffusion measurements, fit parameters of density temperature dependence, Arrhenius and VFT fit parameters for viscosity and self-diffusion coefficient data, fit parameter for homologous series of ln(viscosity) and ln(self-diffusion coefficient), and calculations related to the Stokes–Einstein equation (PDF)

https://doi.org/10.1021/acs.jced.1c00101
J. Chem. Eng. Data 2021, 66, 2480–2500

AUTHOR INFORMATION

Corresponding Authors

Markus M. Hoffmann − *Department of Chemistry and Biochemistry, State University of New York College at Brockport, Brockport, New York 14420, United States;* orcid.org/0000-0002-5469-8665; Phone: + (585) 395-5587; Email: mhoffman@brockport.edu; Fax: + (585) 395-5805

Gerd Buntkowsky − *Institute of Physical Chemistry, Technical University Darmstadt, D-64287 Darmstadt, Germany;* orcid.org/0000-0003-1304-9762; Phone: + 49 6151 16-21116; Email: gerd.buntkowsky@chemie.tu-darmstadt.de; Fax: + 49 6151 16-21119

Authors

Rachel H. Horowitz − *Department of Chemistry and Biochemistry, State University of New York College at Brockport, Brockport, New York 14420, United States*

Torsten Gutmann − *Institute of Physical Chemistry, Technical University Darmstadt, D-64287 Darmstadt, Germany;* orcid.org/0000-0001-6214-2272

Complete contact information is available at: https://pubs.acs.org/10.1021/acs.jced.1c00101

Notes

The authors declare no competing financial interest.

ACKNOWLEDGMENTS

This report is based upon work supported by the National Science Foundation under grant no. [1953428] and the Deutsche Forschungsgemeinschaft (DFG) under grant Bu 911/24-2. The latter included a Mercator fellowship for M.M.H. to support research stays at the Technical University Darmstadt.

REFERENCES

(1) Gullapalli, R. P.; Mazzitelli, C. L. Polyethylene Glycols in Oral and Parenteral Formulations–a Critical Review. *Int. J. Pharm.* **2015**, *496*, 219−239.

(2) Hutanu, D. Recent Applications of Polyethylene Glycols (PEGs) and PEG Derivatives. *Mod. Chem. Appl.* **2014**, *02*, 1.

(3) Kong, X. B.; Tang, Q. Y.; Chen, X. Y.; Tu, Y.; Sun, S. Z.; Sun, Z. L. Polyethylene Glycol as a Promising Synthetic Material for Repair of Spinal Cord Injury. *Neural. Regen. Res.* **2017**, *12*, 1003−1008.

(4) Calvo-Flores, F. G.; Monteagudo-Arrebola, M. J.; Dobado, J. A.; Isac-García, J. Green and Bio-Based Solvents. *Topics Curr. Chem.* **2018**, *376*, 18.

(5) Chen, J.; Spear, S. K.; Huddleston, J. G.; Rogers, R. D. Polyethylene Glycol and Solutions of Polyethylene Glycol as Green Reaction Media. *Green Chem.* **2005**, *7*, 64−82.

(6) Andrade, C. Z.; Alves, L. Environmentally Benign Solvents in Organic Synthesis: Current Topics. *Curr. Org. Chem.* **2005**, *9*, 195−218.

(7) Atashkar, B.; Rostami, A.; Rostami, A.; Zolfigol, M. A. $NiFe_2O_4$ as a Magnetically Recoverable Nanocatalyst for Odourless C-S Bond Formation Via the Cleavage of C-O Bond in the Presence of S_8 under Mild and Green Conditions. *Appl. Organomet. Chem.* **2019**, *33*, E4691.

(8) Bayannavar, P. K.; Kamble, R. R.; Shaikh, S. K. J.; Kumar, S. M.; Kumbar, M. N.; Nesaragi, A. R. L-Proline Catalyzed Multicomponent Domino Reaction in Polyethylene Glycol-400 for Regioselective Synthesis of Pyrazolyl-Tetrahydroindazolones under Microwave Irradiation. *Synth. Commun.* **2019**, *49*, 2005−2016.

(9) Devkate, C. G.; Kola, S. S.; Gaikwad, D. D.; Siddique, M. I. M. Ultrasound Promoted One Pot Synthesis of 1,5-Benzothiazepines Using Polyethylene Glycol (PEG-400). *Int. Res. J. Pharm.* **2018**, *9*, 182−185.

(10) Ghorbani-Choghamarani, A.; Sahraei, R.; Taherinia, Z. Ni(II) Immobilized on Modified Boehmite Nanostructures: A Novel, Inexpensive, and Highly Efficient Heterogeneous Nanocatalyst for Multicomponent Domino Reactions. *Res. Chem. Intermed.* **2019**, *45*, 3199−3214.

(11) Gupta, A. K.; Bharadwaj, M.; Mehrotra, R. Eco-Friendly Polyethylene Glycol-400 as a Rapid and Efficient Recyclable Reaction Medium for the Synthesis of Anticancer Isatin-Linked Chalcones and Their 3-Hydroxy Precursor. *J. Heterocycl. Chem.* **2019**, *56*, 703−709.

(12) McGarvey, P. W.; Hoffmann, M. M. Solubility of Some Mineral Salts in Polyethylene Glycol and Related Surfactants. *Tenside Surfactants Deterg.* **2018**, *55*, 203−209.

(13) Xiong, W. W.; Zhang, Q. Surfactants as Promising Media for the Preparation of Crystalline Inorganic Materials. *Angew. Chem. Int. Ed. Engl.* **2015**, *54*, 11616−11623.

(14) Nobelprize.org The Nobel Prize in Chemistry 2010. https://www.nobelprize.org/prizes/chemistry/2010/heck/lecture/ (accessed Feb. 05, 2021).

(15) Pires, M.; Purificação, S.; Santos, A.; Marques, M. The Role of PEG on Pd- and Cu-Catalyzed Cross-Coupling Reactions. *Synthesis* **2017**, *49*, 2337−2350.

(16) Khanmoradi, M.; Nikoorazm, M.; Ghorbani-Choghamarani, A. Synthesis and Characterization of Pd Schiff Base Complex Immobilized onto Functionalized Nanoporous MCM-41 and Its Catalytic Efficacy in the Suzuki, Heck and Stille Coupling Reactions. *Catal. Lett.* **2017**, *147*, 1114−1126.

(17) Nikoorazm, M.; Ghorbani, F.; Ghorbani-Choghamarani, A.; Erfani, Z. Pd(0)- S-Propyl-2-Aminobenzothioate Immobilized onto Functionalized Magnetic Nanoporous MCM-41 as Efficient and Recyclable Nanocatalyst for the Suzuki, Stille and Heck Cross Coupling Reactions: Fe_3O_4@MCM-41@Pd-SPATB Catalyzed C-C Coupling Reactions. *Appl. Organomet. Chem.* **2018**, *32*, No. e4282.

(18) Nikoorazm, M.; Ghorbani-Choghamarani, A.; Ghobadi, M.; Massahi, S. Pd-SBT@MCM-41: As an Efficient, Stable and Recyclable Organometallic Catalyst for C-C Coupling Reactions and Synthesis of 5-Substituted Tetrazoles. *Appl. Organomet. Chem.* **2017**, *31*, No. e3848.

(19) Hajipour, A. R.; Khorsandi, Z. Immobilized Pd on (*S*)-Methyl Histidinate-Modified Multi-Walled Carbon Nanotubes: A Powerful and Recyclable Catalyst for Mizoroki-Heck and Suzuki-Miyaura C-C Cross-Coupling Reactions in Green Solvents and under Mild Conditions: Immobilized Pd on (*S*)-Methyl Histidinate-Modified MWCNTs. *Appl. Organomet. Chem.* **2016**, *30*, 256−261.

(20) Bakhtyari, A.; Haghbakhsh, R.; Duarte, A. R. C.; Raeissi, S. A Simple Model for the Viscosities of Deep Eutectic Solvents. *Fluid Phase Equilib.* **2020**, *521*, 112662.

(21) Gabriele, F.; Chiarini, M.; Germani, R.; Tiecco, M.; Spreti, N. Effect of Water Addition on Choline Chloride/Glycol Deep Eutectic Solvents: Characterization of Their Structural and Physicochemical Properties. *J. Mol. Liq.* **2019**, *291*, 111301.

(22) Chen, Y. Y.; Walvekar, R.; Khalid, M.; Shahbaz, K.; Gupta, T. C. S. M. Stability and Thermophysical Studies on Deep Eutectic Solvent Based Carbon Nanotube Nanofluid. *Mater. Res. Express* **2017**, *4*, 075028/1−075028/16.

(23) Ghaedi, H.; Ayoub, M.; Sufian, S.; Shariff, A. M.; Lal, B. The Study on Temperature Dependence of Viscosity and Surface Tension of Several Phosphonium-Based Deep Eutectic Solvents. *J. Mol. Liq.* **2017**, *241*, 500−510.

(24) Shekaari, H.; Zafarani-Moattar, M. T.; Mohammadi, B. Liquid-Liquid Equilibria for Benzene/Thiophene + Cyclohexane/Hexadecane + Deep Eutectic Solvents: Data and Correlation. *J. Chem. Eng. Data* **2019**, *64*, 3904−3918.

(25) Ghaedi, H.; Ayoub, M.; Sufian, S.; Shariff, A. M.; Murshid, G.; Hailegiorgis, S. M.; Khan, S. N. Density, Excess and Limiting Properties of (Water and Deep Eutectic Solvent) Systems at Temperatures from 293.15-343.15 K. *J. Mol. Liq.* **2017**, *248*, 378−390.

(26) Mjalli, F. S.; Ahmad, O. Density of Aqueous Choline Chloride-Based Ionic Liquids Analogues. *Thermochim. Acta* **2017**, *647*, 8−14.

(27) Hossain, S. S.; Samanta, A. Solute Rotation and Translation Dynamics in an Ionic Deep Eutectic Solvent Based on Choline Chloride. *J. Phys. Chem. B* **2017**, *121*, 10556−10565.
(28) Branca, C.; Faraone, A.; Magazú, S.; Maisano, G.; Migliardo, P.; Villari, V. Polyethylene Oxide: A Review of Experimental Findings by Spectroscopic Techniques. *J. Mol. Liq.* **2000**, *87*, 21−68.
(29) Borodin, O.; Douglas, R.; Smith, G. D.; Trouw, F.; Petrucci, S. Md Simulations and Experimental Study of Structure, Dynamics, and Thermodynamics of Poly(Ethylene Oxide) and Its Oligomers. *J. Phys. Chem. B* **2003**, *107*, 6813−6823.
(30) Lee, H.; de Vries, A. H.; Marrink, S.-J.; Pastor, R. W. A Coarse-Grained Model for Polyethylene Oxide and Polyethylene Glycol: Conformation and Hydrodynamics. *J. Phys. Chem. B* **2009**, *113*, 13186−13194.
(31) Gaube, J.; Hoechemer, R.; Keil, B.; Pfennig, A. Polydispersity Effects in the System Poly(Ethylene Glycol) + Dextran + Water. *J. Chem. Eng. Data* **1993**, *38*, 207−210.
(32) Cruz, M. S.; Chumpitaz, L. D. A.; Alves, J. G. L. F.; Meirelles, A. J. A. Kinematic Viscosities of Poly(Ethylene Glycols). *J. Chem. Eng. Data* **2000**, *45*, 61−63.
(33) Begum, S. K.; Ratna, S. A.; Clarke, R. J.; Ahmed, M. S. Excess Molar Volumes, Refractive Indices and Transport Properties of Aqueous Solutions of Poly(Ethylene Glycol)s at (303.15-323.15) K. *J. Mol. Liq.* **2015**, *202*, 176−188.
(34) Guo, B.; Zhang, J.; Li, Q.; Li, L.; Ma, H.; Zhang, Q. Solubility of Dilute So2 in the Binary System Poly Ethylene Glycol 300 + Dimethyl Sulfoxide at T = 298.15 K and P = 123.15 Kpa and Mixtures' Excess Properties at T = (298.15, 303.15, 308.15, 313.15, and 318.15) K. *J. Chem. Eng. Data* **2014**, *59*, 2413−2422.
(35) Niu, Y.; Gao, F.; Zhu, R.; Sun, S.; Wei, X. Solubility of Dilute So2 in Mixtures of N,N-Dimethylformamide + Polyethylene Glycol 400 and the Density and Viscosity of the Mixtures. *J. Chem. Eng. Data* **2013**, *58*, 639−647.
(36) Wu, T. Y.; Chen, B. K.; Hao, L.; Lin, Y. C.; Wang, H. P.; Kuo, C. W.; Sun, I. W. Physicochemical Properties of Glycine-Based Ionic Liquid [Quatgly-Oet][Etoso(3)] (2-Ethoxy-1-Ethyl-1,1-Dimethyl-2-Oxoethanaminium Ethyl Sulfate) and Its Binary Mixtures with Poly(Ethylene Glycol) (M(W) = 200) at Various Temperatures. *Int. J. Mol. Sci.* **2011**, *12*, 8750−8772.
(37) Zhang, N.; Zhang, J.; Zhang, Y.; Bai, J.; Huo, T.; Wei, X. Excess Molar Volumes and Viscosities of Poly(Ethylene Glycol) 300+Water at Different Temperatures. *Fluid Phase Equilib.* **2012**, *313*, 7−10.
(38) Bajić, D. M.; Jovanović, J.; Živković, E. M.; Visak, Z. P.; Šerbanović, S. P.; Kijevčanin, M. L. Experimental Measurement and Modelling of Viscosity of the Binary Systems Pyridine or Nicotine with Polyethylene Glycols at T=(288.15−333.15)K. New Unifac−Visco and Asog−Visco Interaction Parameters. *Fluid Phase Equilib.* **2013**, *338*, 282−293.
(39) Vuksanovic, J. M.; Calado, M. S.; Ivanis, G. R.; Kijevcanin, M. L.; Serbanovic, S. P.; Visak, Z. P. Environmentally Friendly Solutions of Liquid Poly(Ethylene Glycol) and Imidazolium Based Ionic Liquids with Bistriflamide and Triflate Anions: Volumetric and Viscosity Studies. *Fluid Phase Equilib.* **2013**, *352*, 100−109.
(40) Sequeira, M. C. M.; Pereira, M. F. V.; Avelino, H. M. N. T.; Caetano, F. J. P.; Fareleira, J. M. N. A. Viscosity Measurements of Poly(Ethyleneglycol) 400 [PEG 400] at Temperatures from 293 K to 348 K and at Pressures up to 50 Mpa Using the Vibrating Wire Technique. *Fluid Phase Equilib.* **2019**, *496*, 7−16.
(41) Wu, T. Y.; Chen, B. K.; Hao, L.; Peng, Y. C.; Sun, I. W. Effect of Temperature on the Physico-Chemical Properties of a Room Temperature Ionic Liquid (1-Methyl-3-Pentylimidazolium Hexafluorophosphate) with Polyethylene Glycol Oligomer. *Int. J. Mol. Sci.* **2011**, *12*, 2598−2617.
(42) Vuksanović, J. M.; Živković, E. M.; Radović, I. R.; Djordjević, B. D.; Šerbanović, S. P.; Kijevčanin, M. L. Experimental Study and Modelling of Volumetric Properties, Viscosities and Refractive Indices of Binary Liquid Mixtures Benzene+PEG 200/PEG 400 and Toluene +PEG 200/PEG 400. *Fluid Phase Equilib.* **2013**, *345*, 28−44.
(43) Ottani, S.; Vitalini, D.; Comelli, F.; Castellari, C. Densities, Viscosities, and Refractive Indices of Poly(Ethylene Glycol) 200 and 400 + Cyclic Ethers at 303.15 K. *J. Chem. Eng. Data* **2002**, *47*, 1197−1204.
(44) Comelli, F.; Ottani, S.; Francesconi, R.; Castellari, C. Densities, Viscosities, Refractive Indices, and Excess Molar Enthalpies of Binary Mixtures Containing Poly(Ethylene Glycol) 200 and 400 + Dimethoxymethane and + 1,2-Dimethoxyethane at 298.15 K. *J. Chem. Eng. Data* **2002**, *47*, 1226−1231.
(45) Živković, N. V.; Šerbanović, S. S.; Kijevčanin, M. L.; Živković, E. M. Volumetric and Viscometric Behavior of Binary Systems 2-Butanol + PEG 200, + PEG 400, + Tetraethylene Glycol Dimethyl Ether, and + N-Methyl-2-Pyrrolidone. *J. Chem. Eng. Data* **2013**, *58*, 3332−3341.
(46) Li, Q.; Sha, F.; Zhao, G.; Yang, M.; Zhao, L.; Zhang, Q.; Zhang, J. Excess Properties for the Binary System of Poly(Ethylene Glycol) 200 + 1,2-Ethanediamine at T = (303.15 to 323.15) K and the System's Spectroscopic Studies. *J. Chem. Eng. Data* **2016**, *61*, 1718−1727.
(47) Comelli, F.; Ottani, S. Excess Enthalpies, Densities, Viscosities, and Refractive Indices of Binary Mixtures Involving Some Poly(Glycols) + Diethyl Carbonate at 308.15 K. *J. Chem. Eng. Data* **2004**, *49*, 970−975.
(48) Francesconi, R.; Bigi, A.; Rubini, K.; Comelli, F. Molar Heat Capacities, Densities, Viscosities, and Refractive Indices of Poly(Ethylene Glycols) + 2-Methyltetrahydrofuran at (293.15, 303.15, and 313.15) K. *J. Chem. Eng. Data* **2007**, *52*, 2020−2025.
(49) Vuksanović, J. M.; Radović, I. R.; Šerbanović, S. P.; Kijevčanin, M. L. Experimental Investigation of Interactions and Thermodynamic Properties of Poly(Ethylene Glycol) 200/400 + Dimethyl Adipate/Dimethyl Phthalate Binary Mixtures. *J. Chem. Eng. Data* **2015**, *60*, 1910−1925.
(50) Adam, O. E.-A. A.; Hassan, A. A. Viscosity, Gibbs Free Energy, and Refractive Indices for Binary Mixtures of O-Cresol + Poly(Ethylene Glycols) at T = 288.15−308.15 K and 96.5 Kpa. *J. Chem. Eng. Data* **2018**, *63*, 3263−3273.
(51) Zhao, T.; Xu, Q.; Xiao, J.; Wei, X. Excess Properties and Spectroscopic Studies for Binary System of Polyethylene Glycol 200 (1) + Dimethyl Sulfoxide (2) at T = (298.15 to 318.15) K. *J. Chem. Eng. Data* **2015**, *60*, 2135−2145.
(52) Aminabhavi, T. M.; Banerjee, K. Density, Viscosity, Refractive Index, and Speed of Sound in Binary Mixtures of Methyl Acetate + Ethylene Glycol or + Poly(Ethylene Glycol) in the Temperature Interval (298.15−308.15) K. *J. Chem. Eng. Data* **1998**, *43*, 852−855.
(53) Trivedi, S.; Pandey, S. Densities of 1-Butyl-3-Methylimidazolium Hexafluorophosphate + Poly(Ethylene Glycol) in the Temperature Range (283.15 to 363.15) K. *J. Chem. Eng. Data* **2011**, *56*, 2168−2174.
(54) Azarang, N.; Movagharnejad, K.; Pirdashti, M.; Ketabi, M. Densities, Viscosities, and Refractive Indices of Poly(Ethylene Glycol) 300 + 1,2-Ethanediol, 1,2-Propanediol, 1,3-Propanediol, 1,3-Butanediol, or 1,4-Butanediol Binary Liquid Mixtures. *J. Chem. Eng. Data* **2020**, *65*, 3448−3462.
(55) Han, F.; Zhang, J.; Chen, G.; Wei, X. Density, Viscosity, and Excess Properties for Aqueous Poly(Ethylene Glycol) Solutions from (298.15 to 323.15) K. *J. Chem. Eng. Data* **2008**, *53*, 2598−2601.
(56) Eliassi, A.; Modarress, H.; Mansoori, G. A. Densities of Poly(Ethylene Glycol) + Water Mixtures in the 298.15−328.15 K Temperature Range. *J. Chem. Eng. Data* **1998**, *43*, 719−721.
(57) Zhang, K.; Yang, J.; Yu, X.; Zhang, J.; Wei, X. Densities and Viscosities for Binary Mixtures of Poly(Ethylene Glycol) 400 + Dimethyl Sulfoxide and Poly(Ethylene Glycol) 600 + Water at Different Temperatures. *J. Chem. Eng. Data* **2011**, *56*, 3083−3088.
(58) Naidu, B. V. K.; Rao, K. C.; Subha, M. C. S. Densities, Viscosities, and Excess Properties for Binary Mixtures of Some Glycols and Polyglycols in N-Methylacetamide at 308.15 K. *J. Chem. Eng. Data* **2003**, *48*, 625−627.
(59) Naidu, B. V. K.; Rao, K. C.; Subha, M. C. S. Densities and Viscosities of Mixtures of Some Glycols and Polyglycols in Dimethyl Sulfoxide at 308.15 K. *J. Chem. Eng. Data* **2002**, *47*, 379−382.
(60) Afzal, W.; Mohammadi, A. H.; Richon, D. Volumetric Properties of Mono-, Di-, Tri-, and Polyethylene Glycol Aqueous Solutions from

https://doi.org/10.1021/acs.jced.1c00101
J. Chem. Eng. Data 2021, 66, 2480−2500

(273.15 to 363.15) K: Experimental Measurements and Correlations. *J. Chem. Eng. Data* **2009**, *54*, 1254−1261.
(61) Awwad, A. M.; Al-Dujaili, A. H.; Salman, H. E. Relative Permittivities, Densities, and Refractive Indices of the Binary Mixtures of Sulfolane with Ethylene Glycol, Diethylene Glycol, and Poly(Ethylene Glycol) at 303.15 K. *J. Chem. Eng. Data* **2002**, *47*, 421−424.
(62) Pereira, M. F. V.; Avelino, H. M. N. T.; Caetano, F. J. P.; Fareleira, J. M. N. A. Viscosity of Liquid Diethylene, Triethylene and Tetraethylene Glycols at Moderately High Pressures Using a Vibrating Wire Instrument. *Fluid Phase Equilib.* **2019**, *480*, 87−97.
(63) Kalaivani, S.; Srikanth, C. K.; Regupathi, I. Densities and Viscosities of Binary and Ternary Mixtures and Aqueous Two-Phase System of Poly(Ethylene Glycol) 2000 + Diammonium Hydrogen Citrate + Water at Different Temperatures. *J. Chem. Eng. Data* **2012**, *57*, 2528−2534.
(64) Barani, A.; Pirdashti, M.; Rostami, A. A. Density, Viscosity, Refractive Index, and Excess Properties of Binary and Ternary Solutions of Poly(Ethylene Glycol), Water, and Dipotassium Tartrate at 298.15 K and Atmospheric Pressure. *J. Chem. Eng. Data* **2017**, *63*, 127−137.
(65) de Ś Costa, B.; Garcia-Rojas, E. E.; Coimbra, J. S. d. R.; Teixeira, J. A.; Telis-Romero, J. Density, Refractive Index, Apparent Specific Volume, and Electrical Conductivity of Aqueous Solutions of Poly(Ethylene Glycol) 1500 at Different Temperatures. *J. Chem. Eng. Data* **2014**, *59*, 339−345.
(66) Mohsen-Nia, M.; Modarress, H.; Rasa, H. Measurement and Modeling of Density, Kinematic Viscosity, and Refractive Index for Poly(Ethylene Glycol) Aqueous Solution at Different Temperatures. *J. Chem. Eng. Data* **2005**, *50*, 1662−1666.
(67) Ebrahimi, S.; Sadeghi, R. Density, Speed of Sound, and Viscosity of Some Binary and Ternary Aqueous Polymer Solutions at Different Temperatures. *J. Chem. Eng. Data* **2015**, *60*, 3132−3147.
(68) McLoughlin, N.; Lee, S. L.; Hähner, G. Temperature Dependence of Viscosity and Density of Viscous Liquids Determined from Thermal Noise Spectra of Uncalibrated Atomic Force Microscope Cantilevers. *Lab Chip* **2007**, *7*, 1057−1061.
(69) Kaur, K.; Juglan, K. C.; Kumar, H. Investigation on Temperature-Dependent Volumetric and Acoustical Properties of Homologous Series of Glycols in Aqueous Sorbitol Solutions. *J. Chem. Eng. Data* **2017**, *62*, 3769−3782.
(70) Rahbari-Sisakht, M.; Taghizadeh, M.; Eliassi, A. Densities and Viscosities of Binary Mixtures of Poly(Ethylene Glycol) and Poly(Propylene Glycol) in Water and Ethanol in the 293.15−338.15 K Temperature Range. *J. Chem. Eng. Data* **2003**, *48*, 1221−1224.
(71) Zafarani-Moattar, M. T.; Tohidifar, N. Effect of Temperature on Volumetric and Transport Properties of Ternary Poly Ethylene Glycol Di-Methyl Ether 2000+Poly Ethylene Glycol 400+Water and the Corresponding Binary Aqueous Solutions: Measurement and Correlation. *Fluid Phase Equilib.* **2013**, *343*, 43−57.
(72) Sahin, M.; Yesil, Z.; Gunel, M.; Tahiroglu, S.; Ayranci, E. Interactions of Glycine with Polyethylene Glycol Studied by Measurements of Density and Ultrasound Speed in Aqueous Solutions at Various Temperatures. *Fluid Phase Equilib.* **2011**, *300*, 155−161.
(73) Kaur, K.; Juglan, K. C.; Kumar, H.; Behal, I. Thermodynamic Interactions Study of Some Ethylene Glycols in Aqueous Aniline Solutions at Different Temperatures: An Acoustical and Volumetric Approach. *J. Chem. Eng. Data* **2018**, *63*, 3237−3251.
(74) Murugesan, T.; Perumalsamy, M. Densities and Viscosities of Polyethylene Glycol 2000 + Salt + Water Systems from (298.15 to 318.15) K. *J. Chem. Eng. Data* **2005**, *50*, 1290−1293.
(75) Silva, R. M. M.; Minim, L. A.; Coimbra, J. S. R.; Rojas, E. E. G.; da Silva, L. H. M.; Minim, V. P. R. Density, Electrical Conductivity, Kinematic Viscosity, and Refractive Index of Binary Mixtures Containing Poly(Ethylene Glycol) 4000, Lithium Sulfate, and Water at Different Temperatures. *J. Chem. Eng. Data* **2007**, *52*, 1567−1570.
(76) Minim, L. A.; Bonomo, R. C. F.; Amaral, I. V.; Reis, M. F. T.; Oliveira, A. A. A.; Minim, V. P. R. Density and Viscosity of Binary and Ternary Mixtures of Poly(Ethylene Glycol) and Poly(Acrylic Acid, Sodium Salt) at Temperatures of (288.15 to 318.15) K. *J. Chem. Eng. Data* **2010**, *55*, 2328−2332.
(77) Regupathi, I.; Govindarajan, R.; Pandian Amaresh, S.; Murugesan, T. Densities and Viscosities of Polyethylene Glycol 6000 + Triammonium Citrate + Water Systems. *J. Chem. Eng. Data* **2009**, *54*, 3291−3295.
(78) Graber, T. A.; Galleguillos, H. R.; Céspedes, C.; Taboada, M. E. Density, Refractive Index, Viscosity, and Electrical Conductivity in the Na_2co_3 + Poly(Ethylene Glycol) + H_2o System from (293.15 to 308.15) K. *J. Chem. Eng. Data* **2004**, *49*, 1254−1257.
(79) Pirdashti, M.; Movagharnejad, K.; Rostami, A. A.; Akbarpour, P.; Ketabi, M. Liquid−Liquid Equilibrium Data, Viscosities, Densities, Conductivities, and Refractive Indexes of Aqueous Mixtures of Poly(Ethylene Glycol) with Trisodium Citrate at Different Ph. *J. Chem. Eng. Data* **2015**, *60*, 3423−3429.
(80) Oh, C. M.; Heng, P. W. S.; Chan, L. W. A Study on the Impact of Hydroxypropyl Methylcellulose on the Viscosity of PEG Melt Suspensions Using Surface Plots and Principal Component Analysis. *AAPS PharmSciTech* **2015**, *16*, 466−477.
(81) Regupathi, I.; Murugesan, S.; Amaresh, S. P.; Govindarajan, R.; Thanabalan, M. Densities and Viscosities of Poly(Ethylene Glycol) 4000 + Diammonium Hydrogen Phosphate + Water Systems. *J. Chem. Eng. Data* **2009**, *54*, 1100−1106.
(82) Graber, T. A.; Galleguillos, H.; Asenjo, J. A.; Andrews, B. A. Refractive Index, Density, and Viscosity in the $Nano_3$ + H_2o + Poly(Ethylene Glycol) System at Various Temperatures. *J. Chem. Eng. Data* **2002**, *47*, 174−178.
(83) Ninni, L.; Burd, H.; Fung, W. H.; Meirelles, A. J. A. Kinematic Viscosities of Poly(Ethylene Glycol) Aqueous Solutions. *J. Chem. Eng. Data* **2003**, *48*, 324−329.
(84) Hoffmann, M. M.; Bothe, S.; Gutmann, T.; Hartmann, F.-F.; Reggelin, M.; Buntkowsky, G. Directly Vs Indirectly Enhanced ^{13}C in Dynamic Nuclear Polarization Magic Angle Spinning NMR Experiments of Nonionic Surfactant Systems. *J. Phys. Chem. C* **2017**, *121*, 2418−2427.
(85) Zagari, J.; Hoffmann, M. M. Polydispersity Analysis of Polyethylene Glycol by Gas and Liquid Chromatography. *Chem. Educ.* **2019**, *24*, 5.
(86) Klimaszewski, K.; Stronka-Lewkowska, E.; Soliwoda, K.; Bald, A. Acoustic and Volumetric Studies on Water + Diethylene Glycol Mixtures in a Wide Temperature Range. Comparison with Mixtures of Water with Tri- and Tetraethylene Glycol. *J. Mol. Liq.* **2016**, *215*, 520−533.
(87) Ali, A.; Ansari, S.; Uzair, S.; Tasneem, S.; Nabi, F. Densities, Ultrasonic Speeds, and Excess Properties of Binary Mixtures of Diethylene Glycol with 1-Butanol, 2-Butanol, and 1,4-Butanediol at Different Temperatures. *Int. J. Thermophys.* **2015**, *36*, 3153−3168.
(88) Li, L.; Zhang, J.; Li, Q.; Guo, B.; Zhao, T.; Sha, F. Density, Viscosity, Surface Tension, and Spectroscopic Properties for Binary System of 1,2-Ethanediamine + Diethylene Glycol. *Thermochim. Acta* **2014**, *590*, 91−99.
(89) Wang, W.; Li, C.; Zhang, N.; Li, M. Excess Molar Volumes and Kinematic Viscosities of Diethylene Glycol + Dimethyl Sulfoxide at T = (298.15, 303.15, 308.15, 313.15 and 318.15) K. *Asian J. Chem.* **2013**, *25*, 5087−5091.
(90) Huo, T.; Zhang, J.; Li, C.; Li, Q.; Liu, Z.; Zhang, T. Hydrogen Bonding and Interaction between Diethylene Glycol and Water: Density, Excess Molar Volume and Spectral Studies. *Asian J. Chem.* **2010**, *22*, 6805−6814.
(91) Catrinciuc, M.; Iulian, O.; Omota, L. M.; Nita, I. Experimental and Calculated Properties in Binary and Ternary Systems with Water, 1,4-Dioxane and Diethylene Glycol at 298.15 K. *Rev. Roum. Chim.* **2006**, *51*, 1011−1018.
(92) Cocchi, M.; Marchetti, A.; Pigani, L.; Sanna, G.; Tassi, L.; Ulrici, A.; Vaccari, G.; Zanardi, C. Density and Volumetric Properties of Ethane-1,2-Diol + Di-Ethylene-Glycol Mixtures at Different Temperatures. *Fluid Phase Equilib.* **2000**, *172*, 93−104.
(93) Aminabhavi, T. M.; Gopalakrishna, B. Density, Viscosity, Refractive Index, and Speed of Sound in Aqueous Mixtures of N,N-Dimethylformamide, Dimethyl Sulfoxide, N,N-Dimethylacetamide, Acetonitrile, Ethylene Glycol, Diethylene Glycol, 1,4-Dioxane,

https://doi.org/10.1021/acs.jced.1c00101
J. Chem. Eng. Data 2021, 66, 2480−2500

Tetrahydrofuran, 2-Methoxyethanol, and 2-Ethoxyethanol at 298.15 K. *J. Chem. Eng. Data* **1995**, *40*, 856−861.
(94) Ren, D.-H.; Fang, S.; Xu, X.-J.; Ding, B. Volumetric Properties and Viscosoties of Acetic Acid with Ethylene Glycol and Diethylene Glycol at Temperatures from 303.15 to 323.15 K. *Chem. Eng. Commun.* **2014**, *201*, 528−544.
(95) Tsierkezos, N. G.; Palaiologou, M. M. Ultrasonic Studies of Liquid Mixtures of Either Water or Dimethyl Sulfoxide with Ethylene Glycol, Diethylene Glycol, Triethylene Glycol, Tetraethylene Glycol, 1,2-Propylene Glycol and 1,4-Butylene Glycol at 298.15 K. *Phys. Chem. Liq.* **2009**, *47*, 447−459.
(96) Hoga, H. E.; Torres, R. B.; Volpe, P. L. O. Thermodynamics Properties of Binary Mixtures of Aqueous Solutions of Glycols at Several Temperatures and Atmospheric Pressure. *J. Chem. Thermodyn.* **2018**, *122*, 38−64.
(97) Almasi, M. Densities and Viscosities of Binary Mixtures Containing Diethylene Glycol and 2-Alkanol. *J. Chem. Eng. Data* **2012**, *57*, 2992−2998.
(98) Begum, S. K.; Clarke, R. J.; Ahmed, M. S.; Begum, S.; Saleh, M. A. Densities, Viscosities, and Surface Tensions of the System Water + Diethylene Glycol. *J. Chem. Eng. Data* **2011**, *56*, 303−306.
(99) Bernal-García, J. M.; Guzmán-López, A.; Cabrales-Torres, A.; Rico-Ramírez, V.; Iglesias-Silva, G. A. Supplementary Densities and Viscosities of Aqueous Solutions of Diethylene Glycol from (283.15 to 353.15) K. *J. Chem. Eng. Data* **2008**, *53*, 1028−1031.
(100) Carvalho, P. J.; Fonseca, C. H. G.; Moita, M.-L. C. J.; Santos, Â. F. S.; Coutinho, J. A. P. Thermophysical Properties of Glycols and Glymes. *J. Chem. Eng. Data* **2015**, *60*, 3721−3737.
(101) Crespo, E. A.; Costa, J. M. L.; Hanafiah, Z. B. M. A.; Kurnia, K. A.; Oliveira, M. B.; Llovell, F.; Vega, L. F.; Carvalho, P. J.; Coutinho, J. A. P. New Measurements and Modeling of High Pressure Thermodynamic Properties of Glycols. *Fluid Phase Equilib.* **2017**, *436*, 113−123.
(102) Silpa, M.; Sasikala, K. A.; Rao, G. S.; Sairam, P. V. S.; Rao, M. V. B. Correlation between Experimental and Theoretical Ultrasonic Velocities in Binary Mixtures of Furfuryl Alcohol with Glycols at 303.15 K. *J. Appl. Chem.* **2019**, *8*, 1417−1425.
(103) Silpa, M.; Sasikala, K. A.; Rao, G. S.; Sairam, P. V. S.; Rao, M. V. B. Acoustic and Volumetric Studies of the Binary Mixtures of Furfuryl Alcohol with Ethylene-, Diethylene- and Triethylene-Glycols at 303.15k. *J. Appl. Chem.* **2019**, *8*, 1363−1370.
(104) Kinart, C. M.; Klimczak, M. Thermodynamic and Structural Properties of Binary Mixtures of Some Glycols with 2-Butoxyethanol at T=(293.15, 298.15 and 303.15) K. *J. Mol. Liq.* **2009**, *148*, 132−139.
(105) Kinart, C. M.; Klimczak, M.; Kinart, W. J. Volumetric and Dielectric Characterization and Analysis of Internal Structure of Binary Mixtures of 2-Ethoxyethanol with Ethylene Glycol, Diethylene Glycol, Triethylene Glycol, and Tetraethylene Glycol at T =(293.15, 298.15 and 303.15) K. *J. Mol. Liq.* **2009**, *145*, 8−13.
(106) Kinart, C. M.; Klimczak, M.; Ćwiklińska, A.; Kinart, W. J. Densities and Excess Molar Volumes for Binary Mixtures of Some Glycols in 2-Methoxyethanol at T =(293.15, 298.15 and 303.15) K. *J. Mol. Liq.* **2007**, *135*, 192−195.
(107) Ćwilińska, A.; Klimczak, M.; Kinart, W. J.; Kinart, C. M. Excess Molar Volumes and Deviations of the Relative Permittivity of the Binary Mixtures of 2-Propoxyethanol with Diethylene, Triethylene, and Tetraethylene Glycols at Various Temperatures. *J. Chem. Thermodyn.* **2008**, *40*, 476−482.
(108) Sagdeev, D. I.; Fomina, M. G.; Mukhamedzyanov, G. K.; Abdulagatov, I. M. Experimental Study of the Density and Viscosity of Polyethylene Glycols and Their Mixtures at Temperatures from 293K to 465K and at High Pressures up to 245MPa. *Fluid Phase Equilib.* **2012**, *315*, 64−76.
(109) Sagdeev, D. I.; Fomina, M. G.; Mukhamedzyanov, G. K.; Abdulagatov, I. M. Experimental Study of the Density and Viscosity of Polyethylene Glycols and Their Mixtures at Temperatures from 293 K to 473 K and at Atmospheric Pressure. *J. Chem. Thermodyn.* **2011**, *43*, 1824−1843.
(110) Francesconi, R.; Castellari, C.; Comelli, F.; Ottani, S. Thermodynamic Study of Binary Mixtures Containing Glycols or Polyethylene Glycols + Benzyl Alcohol at 308.15 K. *J. Chem. Eng. Data* **2004**, *49*, 363−367.
(111) Chen, S.-Y.; Soriano, A. N.; Li, M.-H. Densities and Vapor Pressures of Mixed-Solvent Desiccant Systems Containing {Glycol (Diethylene, or Triethylene, or Tetraethylene Glycol) + Salt (Magnesium Chloride) + Water}. *J. Chem. Thermodyn.* **2010**, *42*, 1163−1167.
(112) Morénas, M.; Douhéret, G. Thermodynamic Behavior of Some Glycol-Water Mixtures. Excess and Partial Volumes. *Thermochim. Acta* **1978**, *25*, 217−224.
(113) Mesquita, F. M. R.; Feitosa, F. X.; Aznar, M.; de Sant'Ana, H. B.; Santiago-Aguiar, R. S. Density, Viscosities, and Excess Properties for Binary Mixtures of Sulfolane + Alcohols and Sulfolane + Glycols at Different Temperatures. *J. Chem. Eng. Data* **2014**, *59*, 2196−2206.
(114) Sastry, N. V.; Patel, M. C. Densities, Excess Molar Volumes, Viscosities, Speeds of Sound, Excess Isentropic Compressibilities, and Relative Permittivities for Alkyl (Methyl, Ethyl, Butyl, and Isoamyl) Acetates + Glycols at Different Temperatures. *J. Chem. Eng. Data* **2003**, *48*, 1019−1027.
(115) Sastry, N. V.; Thakor, R. R.; Patel, M. C. Thermophysical Properties for Diethylene Glycol + Nitrobenzene and Triethylene Glycol + (Chloro-, Bromo-, Nitro-)Benzene Systems at Different Temperatures. *Int. J. Thermophys.* **2008**, *29*, 610−618.
(116) Pal, A.; Singh, W. Speeds of Sound and Viscosities in Aqueous Poly(Ethylene Glycol) Solutions at 303.15 and 308.15 K. *J. Chem. Eng. Data* **1997**, *42*, 234−237.
(117) Kumagai, A.; Mochida, H.; Takahashi, S. Liquid Viscosities and Densities of Hfc-134a (1,1,1,2-Tetrafluoroethane) + Glycol Mixtures. *Int. J. Thermophys.* **1993**, *14*, 45−53.
(118) Muller, E. A.; Rasmussen, P. Densities and Excess Volumes in Aqueous Poly(Ethylene Glycol) Solutions. *J. Chem. Eng. Data* **1991**, *36*, 214−217.
(119) Sun, T.; Teja, A. S. Density, Viscosity, and Thermal Conductivity of Aqueous Ethylene, Diethylene, and Triethylene Glycol Mixtures between 290 K and 450 K. *J. Chem. Eng. Data* **2003**, *48*, 198−202.
(120) Kinart, C. M.; Klimczak, M.; Ćwiklińska, A. Viscosities, Speeds of Sound and Isentropic Compressibilities for Binary Mixtures of 2-Propoxyethanol with Ethylene Glycols. *J. Mol. Liq.* **2010**, *155*, 127−133.
(121) Kinart, C. M.; Klimczak, M.; Kinart, W. Viscosimetric and Structural Properties of Binary Mixtures of 2-Butoxyethanol with Ethylene Glycol, Diethylene Glycol, Triethylene Glycol and Tetraethylene Glycol Systems at T = 293.15, 298.15 and 303.15 K. *Phys. Chem. Liq.* **2011**, *49*, 181−191.
(122) Kinart, C. M.; Klimczak, M.; Maj, M. Viscosity of Binary Mixtures of 2-Ethoxyethanol with Ethylene Glycol, Diethylene Glycol, Triethylene Glycol and Tetraethylene Glycol Systems at T = (293.15, 298.15 and 303.15) K. *Phys. Chem. Liq.* **2009**, *47*, 84−94.
(123) Ćwiklińska, A.; Miecznik, P.; Klimczak, M.; Kinart, C. M. Viscosimetric and Ultrasonic Studies of Intermolecular Interactions of 2-Methoxyethanol with Diethylene Glycol, Triethylene Glycol and Tetraethylene Glycol Binary Mixtures. *Phys. Chem. Liq.* **2008**, *46*, 454−463.
(124) Kinart, C. M.; Maj, M.; Kinart, W. J. Study on the Internal Structure of Some Ethylene Glycols with Sulfolane Binary Mixtures by Means of Measuring Their Viscosities at T = 303.15 K. *Phys. Chem. Liq.* **2009**, *47*, 487−494.
(125) Kinart, C. M.; Maj, M. Viscosities of Ternary Mixtures 2-Alkoxyethanol + Sulfolane + Ethylene Glycols at T = 303.15 K. *Phys. Chem. Liq.* **2011**, *49*, 508−518.
(126) Lee, Y.; Lee, M. Volume Increment Effect on the Photoisomerization of Hemicyanine Dyes in Oligo(Ethylene Glycol)s. *J. Phys. Chem. A* **2013**, *117*, 12878−12883.
(127) Hao, C.; Zhao, L.; Yue, X.; Pang, Y.; Zhang, J. Density, Dynamic Viscosity, Excess Properties and Intermolecular Interaction of Tri-

https://doi.org/10.1021/acs.jced.1c00101
J. Chem. Eng. Data 2021, 66, 2480−2500

ethylene Glycol + N,N-Dimethylformamide Binary Mixture. *J. Mol. Liq.* **2019**, *274*, 730−739.
(128) Qiao, X.; Zhao, T.; Guo, B.; Sha, F.; Zhang, F.; Xie, X.; Zhang, J.; Wei, X. Excess Properties and Spectral Studies for Binary System Tri-Ethylene Glycol + Dimethyl Sulfoxide. *J. Mol. Liq.* **2015**, *212*, 187−195.
(129) Begum, S. K.; Clarke, R. J.; Ahmed, M. S.; Begum, S.; Saleh, M. A. Volumetric, Viscosimetric and Surface Properties of Aqueous Solutions of Triethylene Glycol, Tetraethylene Glycol, and Tetra-ethylene Glycol Dimethyl Ether. *J. Mol. Liq.* **2013**, *177*, 11−18.
(130) Kinart, C. M.; Maj, M.; Bald, A.; Kinart, Z. Volumetric Properties of Ternary Mixtures of Sulfolane with 2-Alkoxyethanols and Ethylene Glycols at T = 303.15k. *J. Mol. Liq.* **2012**, *169*, 87−94.
(131) Kinart, C. M.; Ćwiklińska, A.; Maj, M.; Kinart, W. J. Thermodynamic and Physicochemical Properties of Binary Mixtures of Sulfolane with Ethylene Glycol, Diethylene Glycol, Triethylene Glycol, and Tetraethylene Glycol Systems at 303.15k. *Fluid Phase Equilib.* **2007**, *262*, 244−250.
(132) Guo, Z.; Zhang, J.; Zhang, T.; Li, C.; Zhang, Y.; Bai, J. Liquid Viscosities, Excess Properties, and Viscous Flow Thermodynamics of Triethylene Glycol + Water Mixtures at T = (298.15, 303.15, 308.15, 313.15, and 318.15) K. *J. Mol. Liq.* **2012**, *165*, 27−31.
(133) Aniya, V.; Singh, A.; De, D.; Reddy, R.; Satyavathi, B. Experimental Isobaric Vapor-Liquid Equilibrium at Sub-Atmospheric and Local Atmospheric Pressures, Volumetric Properties and Molar Refractivity from 293.15 to 313.15 K of Water + Triethylene Glycol. *Fluid Phase Equilib.* **2015**, *405*, 132−140.
(134) Valtz, A.; Teodorescu, M.; Wichterle, I.; Richon, D. Liquid Densities and Excess Molar Volumes for Water + Diethylene Glycolamine, and Water, Methanol, Ethanol, 1-Propanol + Triethylene Glycol Binary Systems at Atmospheric Pressure and Temperatures in the Range of 283.15-363.15 K. *Fluid Phase Equilib.* **2004**, *215*, 129−142.
(135) Steele, W. V.; Chirico, R. D.; Cowell, A. B.; Knipmeyer, S. E.; Nguyen, A. Thermodynamic Properties and Ideal-Gas Enthalpies of Formation for Methyl Benzoate, Ethyl Benzoate, (R)-(+)-Limonene, Tert-Amyl Methyl Ether, Trans-Crotonaldehyde, and Diethylene Glycol. *J. Chem. Eng. Data* **2002**, *47*, 667−688.
(136) Klimaszewski, K.; Stronka-Lewkowska, E.; Abramczyk, K.; Bald, A. Acoustic and Volumetric Studies on (Triethylene Glycol + Water) Mixtures in a Wide Temperature Range. *J. Chem. Thermodyn.* **2015**, *89*, 212−222.
(137) Almasi, M. Thermophysical and Transport Properties of Binary Mixtures Containing Triethylene Glycol and Alcohols at Different Temperatures. *J. Therm. Anal. Calorim.* **2016**, *124*, 399−405.
(138) Chen, X.; Li, H.; Guo, F. Measurement and Correlation of Densities and Viscosities of Thiourea in Triglycol Solution Using Vtf Equation. *Russ. J. Phys. Chem. A* **2010**, *84*, 2262−2267.
(139) Pande, R.; Kalamse, G. M. Studies of Alcohol-Amine Complexation by Dielectric Measurements. *Asian J. Chem.* **2005**, *17*, 1794−1798.
(140) Farag, F. M.; Tawfik, S. M. Study the Effect of Chemical Structures of Solvent on the Excess Free Energies of Solution. *J. Appl. Sci. Res.* **2009**, *5*, 605−612.
(141) Fordyce, R.; Lovell, E. L.; Hibbert, H. Studies on Reactions Relating to Carbohydrates and Polysaccharides. Lvi. The Synthesis of the Higher Polyoxyethylene Glycols. *J. Am. Chem. Soc.* **1939**, *61*, 1905−1910.
(142) Filippov, A.; Azancheev, N.; Taher, M.; Shah, F. U.; Rabét, P.; Glavatskih, S.; Antzutkin, O. N. Self-Diffusion and Interactions in Mixtures of Imidazolium Bis(Mandelato)Borate Ionic Liquids with Polyethylene Glycol: (1) H NMR Study. *Magn. Reson. Chem.* **2015**, *53*, 493−497.
(143) Filippov, A.; Azancheev, N.; Gibaydullin, A.; Bhattacharyya, S.; Antzutkin, O. N.; Shah, F. U. Dynamic Properties of Imidazolium Orthoborate Ionic Liquids Mixed with Polyethylene Glycol Studied by NMR Diffusometry and Impedance Spectroscopy. *Magn. Reson. Chem.* **2018**, *56*, 113−119.
(144) Wu, T.-Y.; Su, S.-G.; Chiu, C.-L.; Kuo, C.-W.; Tung, Y.-H. Impact of Polyethyleneglycol Addition on Diffusion Coefficients in Binary Ionic Liquid Electrolytes Composed of Dicationic Ionic Liquid and Polyethyleneglycol. *Magn. Reson. Chem.* **2018**, *56*, 86−94.
(145) Van Geet, A. L. Calibration of the Methanol and Glycol Nuclear Magnetic Resonance Thermometers with a Static Thermister Probe. *Anal. Chem.* **1968**, *40*, 2227−2229.
(146) Jerschow, A.; M̈ller, N. 3D Diffusion-Ordered TOCSY for Slowly Diffusing Molecules. *J. Magn. Reson. A* **1996**, *123*, 222−225.
(147) Jerschow, A.; M̈ller, N. Suppression of Convection Artifacts in Stimulated-Echo Diffusion Experiements. Double-Stimulated-Echo Experiments. *J. Magn. Reson.* **1997**, *125*, 372−375.
(148) Nicolay, K.; Braun, K. P. J.; de Graaf, R. A.; Dijkhuizen, R. M.; Kruiskamp, M. J. Diffusion NMR Spectroscopy. *NMR Biomed.* **2001**, *14*, 94−111.
(149) Tasaki, K. Poly(Oxyethylene)-Water Interactions: A Molecular Dynamics Study. *J. Am. Chem. Soc.* **1996**, *118*, 8459−8469.
(150) Lee, H.; Venable, R. M.; Mackerell, A. D., Jr.; Pastor, R. W. Molecular Dynamics Studies of Polyethylene Oxide and Polyethylene Glycol: Hydrodynamic Radius and Shape Anisotropy. *Biophys. J.* **2008**, *95*, 1590−1599.
(151) Egorov, G. I.; Makarov, D. M.; Kolker, A. M. Densities and Volumetric Properties of Ethylene Glycol + Dimethylsulfoxide Mixtures at Temperatures of (278.15 to 323.15) K and Pressures of (0.1 to 100) Mpa. *J. Chem. Eng. Data* **2010**, *55*, 3481−3488.
(152) Hayamizu, K.; Tsuzuki, S.; Seki, S.; Fujii, K.; Suenaga, M.; Umebayashi, Y. Studies on the Translational and Rotational Motions of Ionic Liquids Composed of N-Methyl-N-Propyl-Pyrrolidinium (P13) Cation and Bis(Trifluoromethanesulfonyl)Amide and Bis-(Fluorosulfonyl)Amide Anions and Their Binary Systems Including Lithium Salts. *J. Chem. Phys.* **2010**, *133*, 194505/1−194505/13.

https://doi.org/10.1021/acs.jced.1c00101
J. Chem. Eng. Data 2021, 66, 2480−2500